1964

A Study of Satellite Amplitude Scintillation and its Correlation with Radio Star Scintillation

William Beeuwkes Shuler
College of William & Mary - Arts & Sciences

A STUDY OF SATELLITE AMPLITUDE SCINTILLATION AND ITS CORRELATION WITH RADIO STAR SCINTILLATION

A Thesis

Presented to

The Faculty of the Department of Physics

The College of William and Mary in Virginia

In Partial Fulfillment

Of the Requirements for the Degree of

Master of Arts

By

William B. Shuler

May 1964

APPROVAL SHEET

This thesis is submitted in partial fulfillment of the requirements for the degree of

Master of Arts

W. B. Shuler

Author

Approved, May 1964:

James D. Lawrence Jr.

James D. Lawrence, Jr., Ph.D.

Melvin A. Pittman

Melvin A. Pittman, Ph.D.

D. E. McLennan

Donald E. McLennan, Ph.D.

Frederic R. Crownfield Jr.

ACKNOWLEDGMENTS

The author wishes to express his appreciation to Dr. J. D. Lawrence under whose direction this research was performed; also the author wishes to thank Dr. Donald E. McLennan and Dr. Melvin Pittman for their reading and criticism of the manuscript. The author extends his special thanks to his wife, Jeanne, for her encouragement and help in typing the manuscript. This investigation was supported by the National Science Foundation under research grant number NSF-G-16495.

TABLE OF CONTENTS

	Page
ACKNOWLEDGMENTS	iii
ABSTRACT	v
INTRODUCTION	2
THE IONOSPHERE	8
EQUIPMENT	15
EXPERIMENTAL PROCEDURE	31
EXPERIMENTAL RESULTS	37
CONCLUSIONS	58
REFERENCES	60

ABSTRACT

Measurements of the signal fluctuations of the cosmic source Cassiopeia A and artificial earth satellite Transit IV A were recorded simultaneously at Williamsburg, Virginia for the period July 1963 through August 1963. A linear correlation analysis done on the accumulated data indicates that no linear correlation exists between radio star and satellite scintillation activity.

To investigate the possibility of a general correlation between these two phenomena, published features of radio star scintillation activity and satellite studies done at the College of William and Mary are compared. Latitudinal, diurnal, and elevation angle effects seem to indicate that there is a good general correlation between radio star and satellite scintillation. Because seasonal effects and variations with the solar cycle are not fully understood for both star and satellite scintillation phenomena, no direct comparison is possible.

A STUDY OF SATELLITE AMPLITUDE SCINTILLATION AND ITS CORRELATION WITH RADIO STAR SCINTILLATION

INTRODUCTION

Early investigations of the ionosphere were conducted by bottom side sounding techniques with access to only the lowest regions. With the discovery of discrete sources of cosmic radio emission by Jansky[1] the upper regions of the ionosphere were made available for observation. In 1946, Hey, Parsons, and Phillips,[2] observed short period irregular fluctuations in the amplitude of noise power from the cosmic source Cygnus A at a wavelength of five meters. At that time these fluctuations were attributed to variable emission of the source. In 1948 Smith[3] and Little and Lovell[4] separately conducted a series of experiments showing conclusively that these fluctuations were local in origin and probably were produced by changes in the index of refraction of the ionosphere. A survey of subsequent observations is given by Booker[5] in which he notes an increase of scintillation with inreasing zenith angle, a maximum of scintillation at midnight, and a good correlation between amplitude scintillation and spread F reflections.

The advent of artificial earth satellites has made possible a more comprehensive and direct study of the irregularities responsible for scintillation phenomena. Extensive studies of the ionosphere using signals transmitted by artificial earth satellites have been carried out by Yeh and Swenson[6] and many others. A summary of these investigations, given by Lawrence and Martin,[7] indicates the same general trends as those observed by Booker[5] for star scintillation.

It would appear then that a simultaneous study of the ionosphere by satellite and radio star observation would offer a more complete and comprehensive method of investigation than either method by itself. To further investigate the possibility of correlation between satellite and star scintillation Slee[8] and Parthasarathy and Reid[9] have made simultaneous observations.

Slee observed the 108 Mc/s radio signal transmitted by the 1958 alpha from February 1 until March 10, 1958 at Sydney, Australia. At the same time observations of the cosmic radio sources Hydra-A, Virgo-A and Taurus-A were made at the nearby frequency of 85.5 Mc/s. The zenith angles of the cosmic sources ranged from 22° to 56° and corresponded approximately with the same range of zenith angles of 1958 alpha. The scintillation activity of the satellite signal on 31 nights (82 transits) is summarized in Figure 1. The vertical lines show the range of scintillation indices observed on each night. For comparison, the nights of high cosmic source scintillation (index ≥ 0.3) are indicated on the graph by the average cosmic source index. Table 1 gives a general comparison of star and satellite indices. From these results, Slee concluded that there is no one-to-one correspondence between the indices for the satellite and the cosmic sources, but that there is a general relation. The average duration of the satellite fluctuation peaks (less than one second) is consistent with that predicted for a source with angular velocity about 100 times that of a cosmic radio source. He also concludes that the region of the ionosphere causing scintillation is below 350 km because at the satellite's perigee of 350 km there was no marked decrease in scintillation. Further, there seemed to be correlation between time of appearance of satellite scintillation and the occurrences of fluctuations of the cosmic radio source.

Parthasarathy and Reid[9] have made similar observations; however, their results seem to be somewhat less conclusive. The 20.005 Mc/s signal of 1958 delta 2 (Sputnik III) was recorded at College, Alaska (64.9°N, 147.8°W) from August to October, 1958. At the same time the Geophysical Institute recorded radio star scintillation continuously at frequencies of 223 and 456 Mc/sec, and a rough comparison of these records with satellite records was carried out. According to Parthasarathy and Reid, the scintillation amplitude should increase as the square of the wavelength, thus they assert that even a trace of scintillation at 223 Mc/s would produce violent fluctuation in the 20 Mc/s signal. Their observations reveal that on many occasions the satellite signal showed less than 5 percent fluctuation while the 223 Mc/s fluctuations amounted to as much as 30 to 50 percent. From these results the authors conclude that either the region responsible for scintillation phenomena is very sharply bounded in the horizontal plane, or that the satellite 1958 delta 2 was moving below the irregularities. They also note that in view of the excessive height of 1958 delta 2 (greater than 600 km) the latter conclusion implies a height for the scintillation region greater than that currently accepted.

From the results of these two studies it would seem reasonable to conclude that due to the random distribution of irregularities in the ionosphere a one-to-one correspondence between the satellite and star fluctuation indices would not be expected. Since, however, the star and satellite signals see the same irregularities over the observer's region of the sky, a general correlation should be expected.

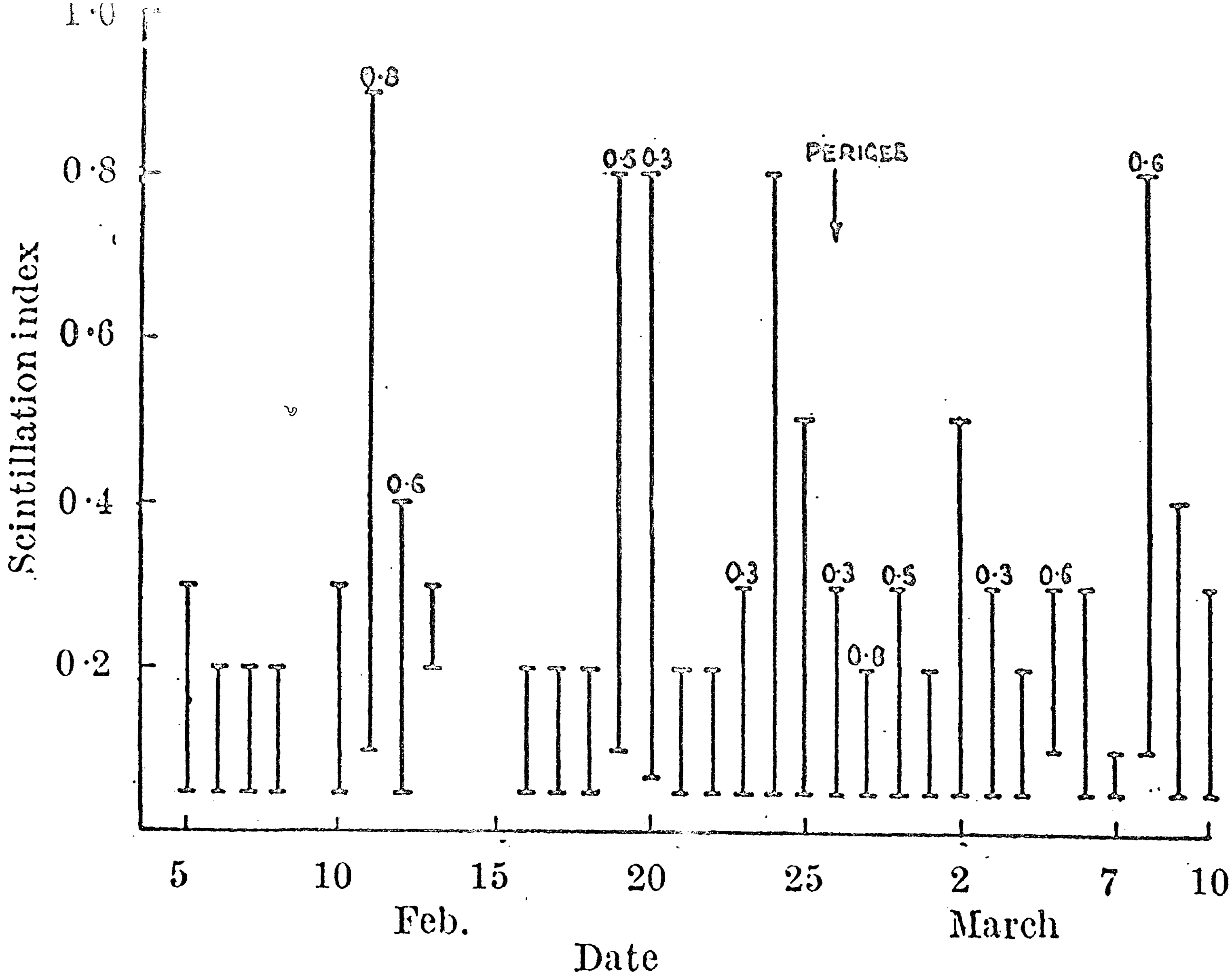

Chart showing the range of the satellite's scintillation index for each night's recording. The numbers in the diagram give the values of the average scintillation index for cosmic radio sources for nights when its value $\geqslant$ 0·3. The date of perigee is marked by the arrow

FIGURE I (Slee)

Table 1. CORRELATION BETWEEN THE FLUCTUATION INDEX FOR THE COSMIC RADIO SOURCES HYDRA-A, VIRGO-A AND TAURUS-A AND THAT FOR THE SATELLITE 1958α

Cosmic source index	Satellite index	
	High	Low
High	10 days	1 day
Low	8 days	9 days

(Slee)

THE IONOSPHERE

The ionosphere, as proposed by Watson Watt, is the region of the earth's atmosphere in which there are free electrons in significant numbers. Specifically a committee of the Institute of Radio Engineers[10] defines it as the part of the earth's upper atmosphere where ions and electrons are present in quantities sufficient to affect the propagation of radio waves. At present its lower limit is thought to be about 50 km and its upper limit above 500 km. The ionosphere consists of regions arranged approximately in horizontally stratified layers denoted by the letters D, E, and F. Early observations indicated that these layers were defined by sharp peaks in the electron distributions as a function of height. Recently, however, rocket measurements have indicated that these layers are not necessarily defined by maxima in the electron density; frequently they are marked only by a ledge where the gradient is small. In order to avoid inconsistencies, the committee[10] recommends the ionosphere be divided into regions called D, E, and F, so that the part of the ionosphere below 90 km is called the D region, that between 90 and 160 km the E region, and that above 160 km the F region. The electron density is greatest above 100 km rising to a maxima of about 10^5 cm^{-3} at the "peak" of the E layer (about 120 km) and to a greater maximum, 10^6 cm^{-3} at the peak of the F_2 layer (about 300 km). Figure 2 gives a plot of electron density as a function of height for an average daytime ionosphere for the year 1962 while Figure 3 gives the diurnal variation of the electron density.

D Region

The D region exists only during the day, merging into the E region at night. This region, being the lowest, has a much higher particle density than the others giving rise to a higher collision frequency. Due to the high collision frequency medium wavelength radio waves are appreciably absorbed. Only very low frequency (3-30 Kc/s) echos can be obtained from the D region using relatively large power.

Aiken,[11] in a preliminary study, has concluded that solar X-rays and ultraviolet radiation do not penetrate the D region noticably at sunrise. The major portion of the upper normal D region is produced at layer sunrise by attenuated Lyman alpha radiation. Also the action of cosmic rays and photodetachment from negative ions leads to a build up of the lowest portion of the D region reaching a maximum daytime value within a short time of layer sunrise. This gives rise to a D region consisting of two layers differentiated by their origin. In a late study Nicolet and Aiken[12] have conducted a theoretical study of the D region concluding that ionization processes correspond to (1) a normal ionization of nitric oxide by Lyman alpha with a resultant ionization peak at 85 km, (2) cosmic radiation as the primary ionizing agent below 70 km, and to ionization by X-rays of 2 kev or more varying with solar activity. In addition to the two normal layers described by Aiken in his preliminary study, they predict a complete transformation of the shape of the normal D layer due to the effect of solar flares. They also assert that the D region is not a downward elongation of the E region, as previously suspected,[13] because the tail of the E layer is due to ionization by X-rays of $\lambda > 31$ Å and, therefore, is formed by processes other than those that create the D region.

E Region

The E region is situated approximately in the middle of the ionosphere. The maximum ion density is about 10^5 electrons per cubic centimeter (occuring at about 120 km) subject to variation of about 50 to 60 percent in the course of the sunspot cycle. This layer, like the D layer, is also closely associated with the sun. The electron density increases from sunrise reaching a noon maximum, then decreases until sunset. It is not certain whether this layer exists during the night. Rocket measurements have revealed that the primary ionizing agents for the E layer are soft X-rays. N_2^+, O_2^+, and O^+ appear in greatest abundance in this region. Dissociative recombination between electrons and positive molecular ions account for the dissappearance of electrons in the E layer.

Sporadic E

At times measurements of abrupt increase in the critical frequency reveal distribution of intense ionization between 90 and 120 km. Because of its irregular nature this region is referred to as the sporadic E layer. Its appearance seems entirely unpredictable and its structure and origin are not known. Solar corpuscular radiation, meteors, thunderstorms, ionospheric currents, and winds and turbulence are all thought to contribute to the formation of this layer. Three models have been proposed to account for experimental observations: a thin horizontal layer of high electron density superimposed on the normal E layer,[14] a steep gradient occuring in the upper or lower part of the normal E region, and blobs of appreciably different electron density embedded in the normal E layer.

F Region

The F region is that region occuring above 160 km. It is subdivided into two layers, F_1 and F_2. The F_1 peak occurs at 160 km with an electron density of 2.5×10^5 electrons/cm^3 during the day and merges up into the F_2 layer at night. During the dark hours the F_2 peak rises to a height of about 350 km. According to Martyn[15] the F_2 ionization peak (5×10^5 electrons/cm^3) occurs at an average height of about 250 km during the day, thus the F_1 region is closer to the E region than it is to the F_2 region. At sunspot minimum, however, there is reason to believe that both the F_1 and F_2 regions are formed by the same solar ionizing radiation (ultraviolet and X-ray radiation). The F_2 region is perturbed by both solar and lunar tidal influences as well as by conditions associated with magnetic storms. These disturbances usually result in a decrease in electron density and an increase in the height of the layer. Occasionally, reflected ionosonde echos are diffuse and broader than the incident transmitted pulse indicating reflection from an anisotropic region, a phenomena termed spread

F. It is thought that the spread F region consists of randomly distributed "blobs" of electron densities differing from their surroundings. Yeh and Swenson[6] observed good correlation between the night time scintillations of satellites 1957 δ_2 and 1958 α_2 and the occurrence of ionospheric spread F. Booker[5] also observed similarities in the diurnal variation of spread F and radio star scintillation. Both exhibit a midnight maximum and are chiefly a night time phenomena. The results of a later, more complete study by Briggs[16] seem to indicate a negative correlation between radio star scintillation and spread F phenomena. The data accumulated in this study extend over one complete solar cycle from 1949 to 1960. These data show that the scintillation effect is greatest at sunspot maximum, while spread F echos occur more frequently at sunspot minimum. It is concluded that at sunspot maximum the ionospheric irregularities which cause radio star scintillation must be mainly above the level of maximum ionization of the F region.

The upper limit of the F region is generally taken to occur where O^+ ceases to be the predominate ion. This region is accessible only by "top side" sounding satellites.

AVERAGE DAYTIME IONOSPHERE

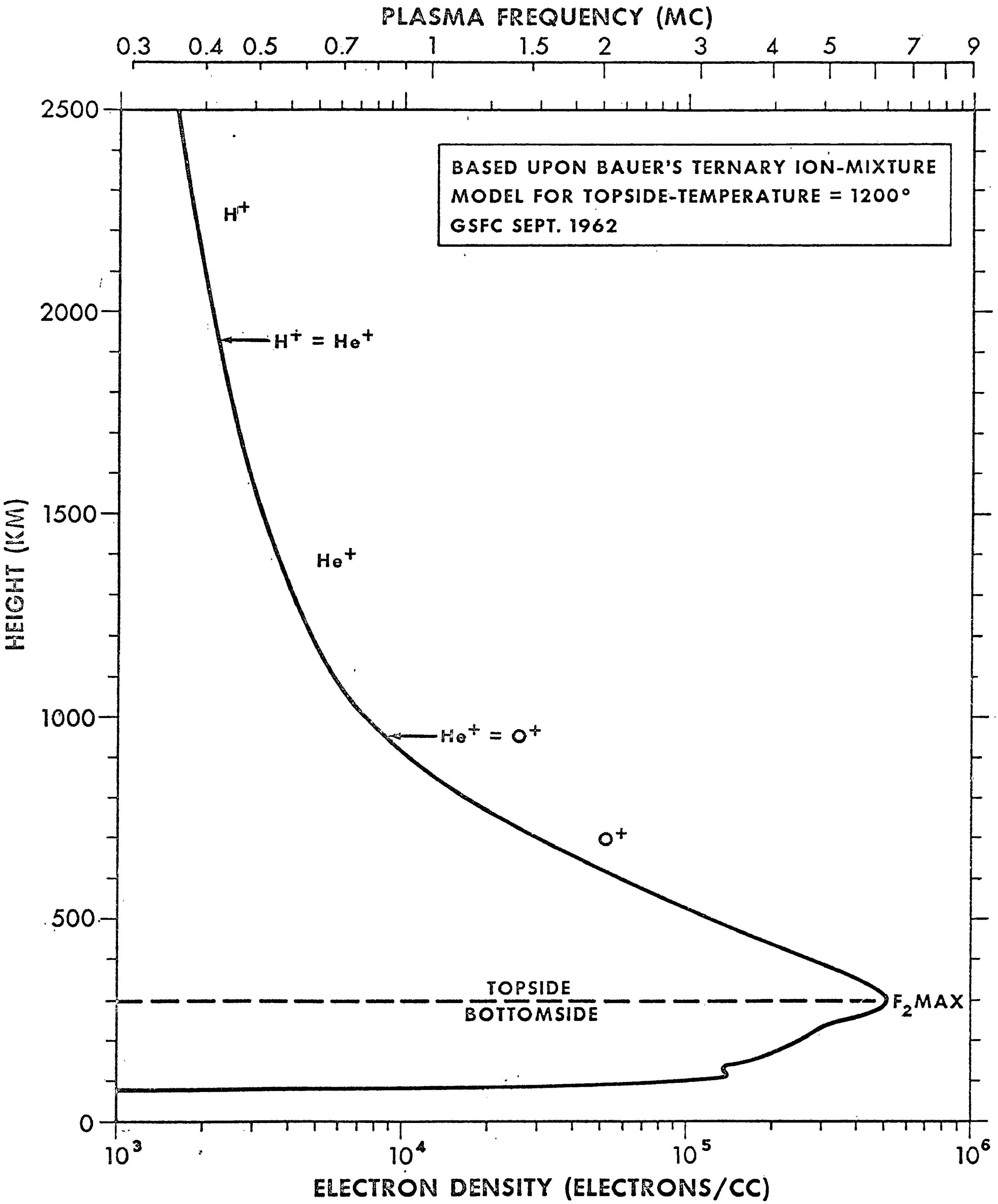

FIGURE 2

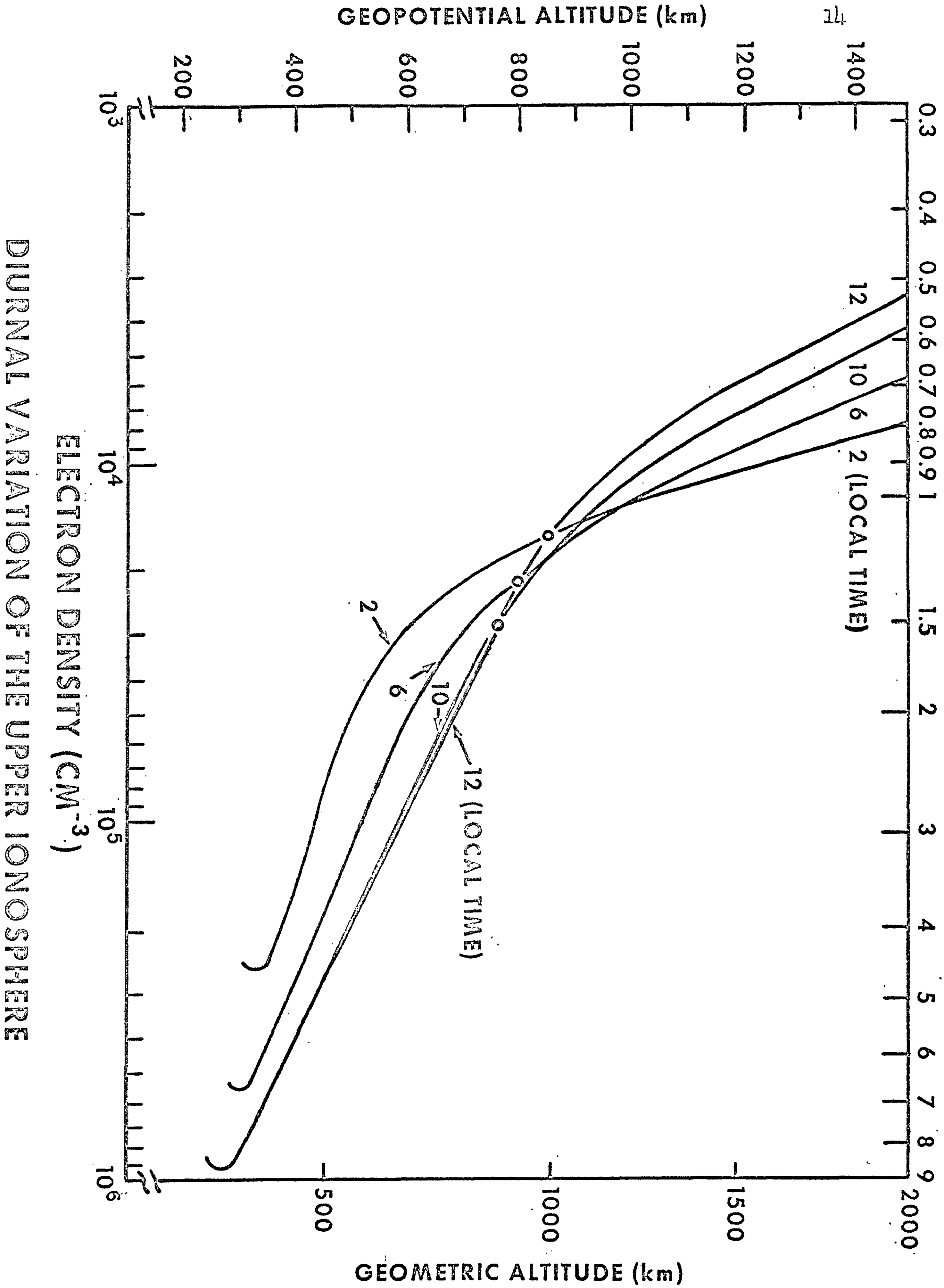
GEOPOTENTIAL ALTITUDE (km)
200
400
600
800
1000
1200
1400
0.3
0.4
0.5
0.6
0.7
0.8
0.9
1
1.5
2
3
4
5
6
7
8
9
12
10
6
2 (LOCAL TIME)
2
6
10
12 (LOCAL TIME)
10^3
10^4
10^5
10^6
ELECTRON DENSITY (CM^{-3})
DIURNAL VARIATION OF THE UPPER IONOSPHERE
500
1000
1500
2000
GEOMETRIC ALTITUDE (km)

FIGURE 3

EQUIPMENT

The equipment used in this study consists of radio star and artificial earth satellite receiving equipment. Cassiopeia A was observed at a frequency of 39 Mc/s while Transit IV A was observed at 54 Mc/s.

Radio Star Receiving Equipment

A Ryle-Vonberg system[17] was used to record fluctuations in the cosmic radio source Cassiopeia A. The receiving equipment is shown in block diagram in Figure 4, and in detail in Figures 5, 6, 7, and 8. The description of this system is due mainly to Hollinger.[18] The general operation of this system may be described as follows: the receiver input is rapidly switched between the aerial and a noise diode used as a calibrated source. The output is then amplified at the switching frequency and rectified in a phase-sensitive detector. The output of the phase detector is used to control the noise diode output so that it is always equal to the signal from the aerial. This forms a null balancing system and the noise diode current is a measure of the received aerial power.

The signal to be measured from the radio source has a roughly constant mean power over the frequency range of interest and is such that any given frequency is randomly related in amplitude and phase to any other frequency.[18] Such a signal is commonly termed white noise. Since the input of the receiver is to be switched between this signal and a comparison source, it is necessary that the comparison source be of similar nature.

The temperature-limited noise diode is such a source. The diode is driven with a sufficiently high voltage between the anode and the filament so that all electrons emitted from the filament are drawn to the anode. Thus the anode current is limited only by the temperature of the filament. The mean-square value of the noise current in a bandwidth Δf is

$$\overline{i_n^2} = 2eI\Delta f$$

where e is the electronic charge, and I is the mean anode current. If this current is fed through a resistor the maximum power available at the input of the receiver will be

$$P = \left(\frac{\overline{i_n^2}}{4}\right) R = \frac{eIR\Delta f}{2}$$

where R is the resistance. Nyquist[19] has shown that the thermal noise power available in a frequency bandwidth Δf from any passive network at absolute temperature T is

$$P = kT\Delta f$$

where K is Boltzmann's constant. Thus the resistor, operating at temperature T_o, will contribute its own thermal noise power,

$$P_o = kT_o\Delta f.$$

Therefore the equivalent thermal power at the input of the receiver will be

$$P_e = kT_o\Delta f + \frac{eIR\Delta f}{2}$$

which is a linear function of the anode current. This defines an equivalent temperature,

$$T_e = T_o + \frac{eIR}{2k}.$$

Thus by employing a temperature limited noise diode it is possible to generate a noise power comparable to the power received at the aerial, which is relatively high at very high frequencies. Obviously an attempt to use the Johnson noise power generated by a resistor is impractical due to the necessarily high resistance temperature, of the order of thousands of degrees, dictated by Nyquist's relation.

The aerial and the noise diode are alternately connected to the input of the receiver by means of an electronic switch. Thus the receiver input will be some mean noise power modulated at the switching frequency; the amount of modulation will be proportional to the power difference between the aerial and the noise diode. This signal is fed to a superheterodyne receiver, and the detected signal is the input to a high Q audio amplifier which amplifies at the switching or modulation frequency. The output of the audio amplifier is independent of the level of the mean power signal and proportional to the modulation component. This output is fed to a phase-sensitive detector which is driven at the same frequency as the switch and phase locked with it. The modulation component is rectified, while all other noise or signal at the switching frequency will have a random phase with respect to the detector and will average to zero. The output of the phase detector is thus a d.c. voltage proportional to the difference between the aerial and noise diode signals. This d.c. voltage is used in a negative feedback fashion to control the diode filament voltage and make the diode signal equal to the aerial signal. The receiver, used in this manner, is a null detector which maintains equal noise diode and aerial signals. The noise diode current is recorded on a fixed span Varian G-10 recorder and is a measure of the received aerial power.

A more detailed description of these components follows, and once again, is due mainly to Hollinger.

The aerial is a five-element "yagi" designed at 39 Mc/sec. It has a gain of six over an iostropic standard and a beam width of approximately 45° between half power points.

All B+ power is supplied by a Sola constant voltage d.c. power supply giving 0.6 amps at +250 volts. Receiver power is supplied by a vacuum tube regulator at +250 volts from the Sola. A -150 volts d.c. bias supply is incorporated in the control unit. This supply is also used to drive the noise diode.

The preamplifiers are the Cascode grounded grid type with gain from 10 to 15 and noise figures from 2 to 3.

The electronic switch consists of two opposing diodes in the signal leads from the noise diode and the preamplifier. An applied square wave bias alternately renders one conducting while the other is shut off. Thus the receiver input is successively connected to the preamplifier and then to the noise diode at the frequency of the square wave (1000 cps).

The signal is fed from the output of the crystal switch to a superheterodyne receiver where it undergoes one stage of R.F. amplification and is then beat with the third harmonic of a 10.131 Mc/sec crystal controlled oscillator. Following three stages of I.F. amplification, the signal is detected and sent to the audio amplifier. The receiver has a gain of approximately 2×10^5, a bandwidth of approximately 80 Kc/sec and a noise figure of 10 to 15.

The audio amplifier includes a twin-T rejection filter in a feedback loop. Maximum rejection occurs at the switching frequency. The amplifier has a Q of about 12 and a maximum potentiometer tuned gain of about 5000. The minimum signal level capable of amplification is 1 to 2 millivolts.

The signal is fed from the output of the audio amplifier to the phase detector. The phase detector functions as a switch that is opened and closed to ground at the frequency of the driving square wave. When the switch is opened, the signal appears at the integrator where, after integration, it is sent to a cathode follower. The cathode follower provides a means of adjusting the bias of the d.c. amplifier which follows and at the same time prevents loading of the integrator.

The signal from the cathode follower is amplified by a d.c. amplifier with a gain of 15. The d.c. level at the plate, about +150 volts in the operating range, is used to control one leg of an "and" circuit while the other leg is held at a mean level of +150 volts and fed with a 2.5 Kc/sec sine wave from a phase shift oscillator. The junction of the two diodes is essentially at the d.c. amplifier plate potential, and for any 2.5 Kc/sec signal to be passed, it must rise above this potential to render the diode on the 2.5 Kc/sec side conducting. Thus only the higher side of the 2.5 Kc/sec sine wave is passed, and by changing the d.c. amplifier plate potential more or less of the 2.5 Kc/sec signal is passed.

The 2.5 Kc/sec signal passed by the "and" circuit is then amplified by a one-stage a.c. amplifier with a gain of 5. It is then amplified in a power amplifier which drives the filaments of the noise diode.

Thus an increasing signal at the phase detector causes an increase in the noise diode output which brings about a decrease in the potential at the phase detector, thus comprising a negative feedback network.

The plate current from the noise diode is fed through a tuned resonance circuit and two series resistors, while the signal to the crystal switch is inductively coupled out. The resonance circuit provides a means of adjusting the number of milliamperes of diode current equivalent to a given signal.

The signal to be recorded may be taken off either of the two series resistors, thus providing a means of bypassing the low band pass filter. The filter consists of a differentiator followed by an integrator. The differentiator has a time constant of about 60 seconds and removes the large gradual frequency variations. The integrator removes the rapid variations. Bowhill[20] has shown that in order to preserve the amplitude and phase of the signal to within 10%, the time constant must be less than 1/10 of the mean fading period. For the signal of interest the scintillation periods are between 50 and 350 seconds[18]; thus the integrator time constant was chosen to be approximately 5 seconds.

The output of the filter is fed to a cathode follower in order to match impedance with the recorder which follows.

Two potentiometers in the output of the cathode follower allow adjustment of the d.c. zero and the gain of the equipment.

The output of the cathode follower is sent to a Varian G-10 Graphic Recorder, with a response time of about 1 second and a full scale sensitivity of 100 millivolts.

A mechanism is incorporated in the control unit to prevent large signals from saturating the equipment to a point where the system cannot return to normal operation after the signal is removed. A large signal can drive the plate of the d.c. amplifier to a very low potential thus applying a large reverse voltage across the diode in the d.c. amplifier side of the "and" circuit. This will reduce the impedance of the diode below the value it has in the operating range. This increases the loading effect of the circuit on the 2.5 Kc/sec oscillator, and thus reduces the amplitude of its output and decreases the noise diode output from what it would be for a smaller signal. This process constitutes a "knee" in the signal response of the unit, and once over this "knee", it cannot return to normal operation. This is prevented by restricting the cathode of the cathode follower bias tube from going to very high potentials despite a high potential on its grid.

Essentially this is done by connecting the two cathodes by a diode placed in such a sense that it conducts when the bias potential rises above the set potential from the cathode of the power amplifier. In this manner the bias is prevented from rising much above the desired level.

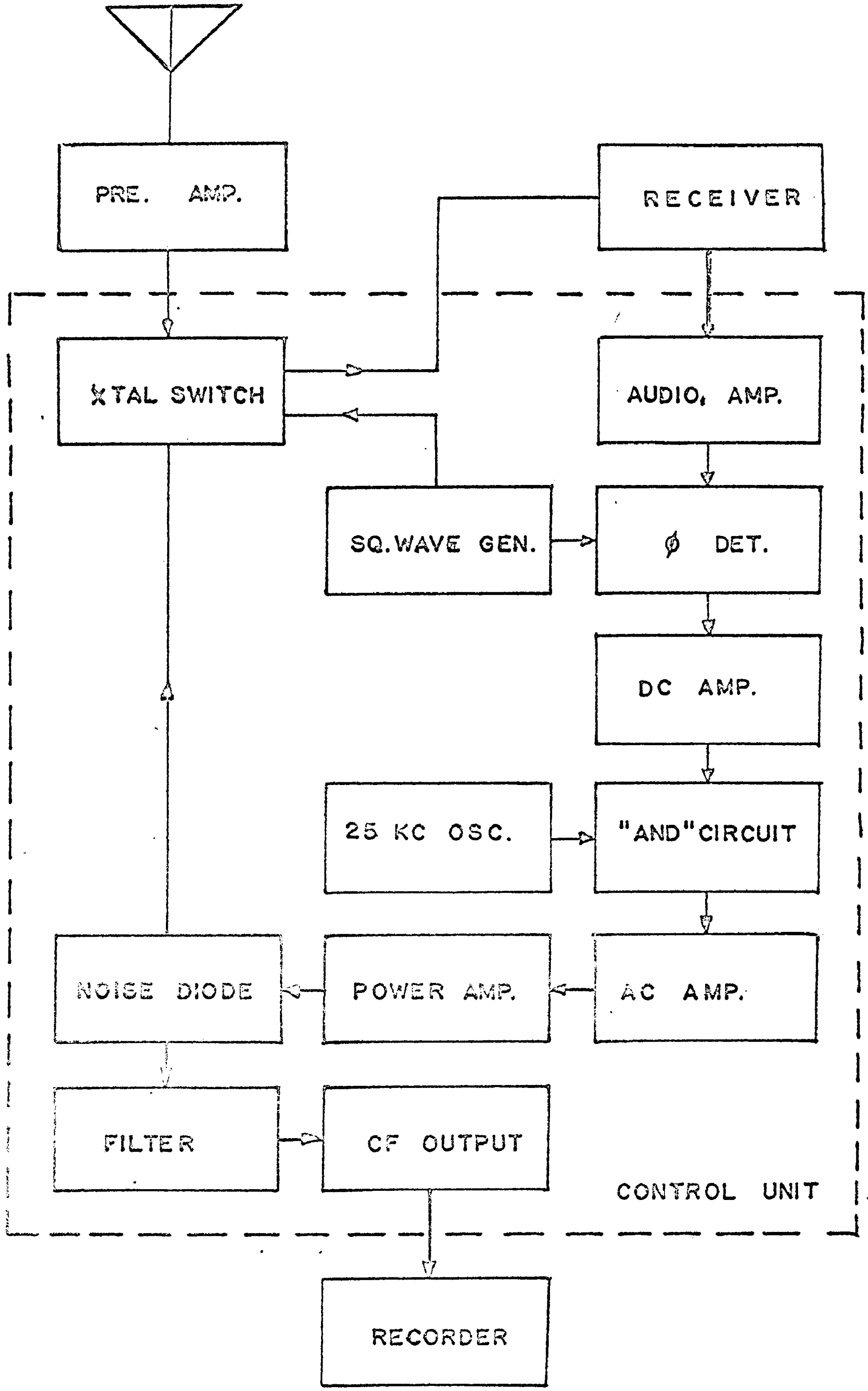

BLOCK DIAGRAM OF EQUIPMENT

FIGURE 4

PRE-AMPLIFIER

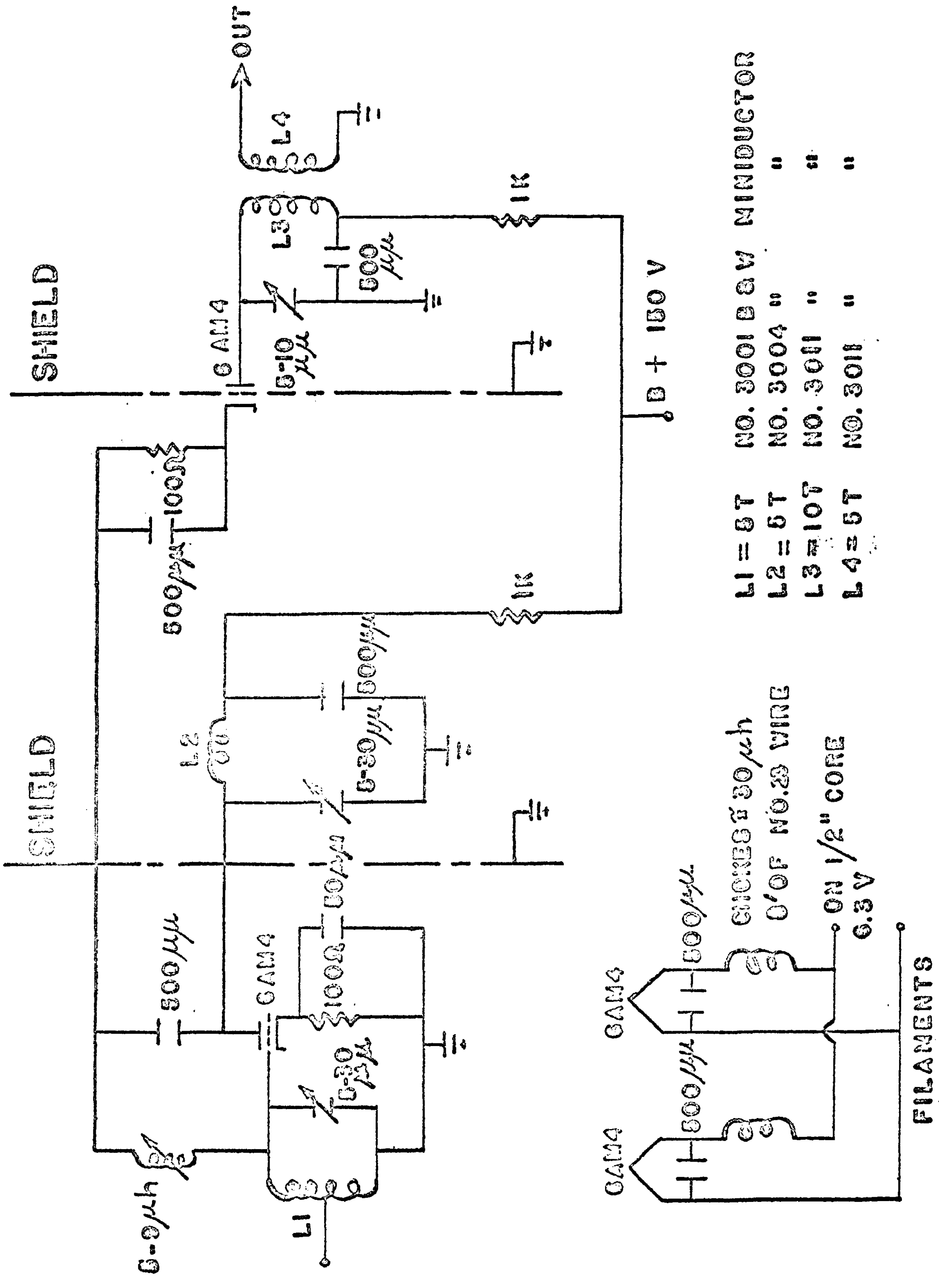

FIGURE 5.

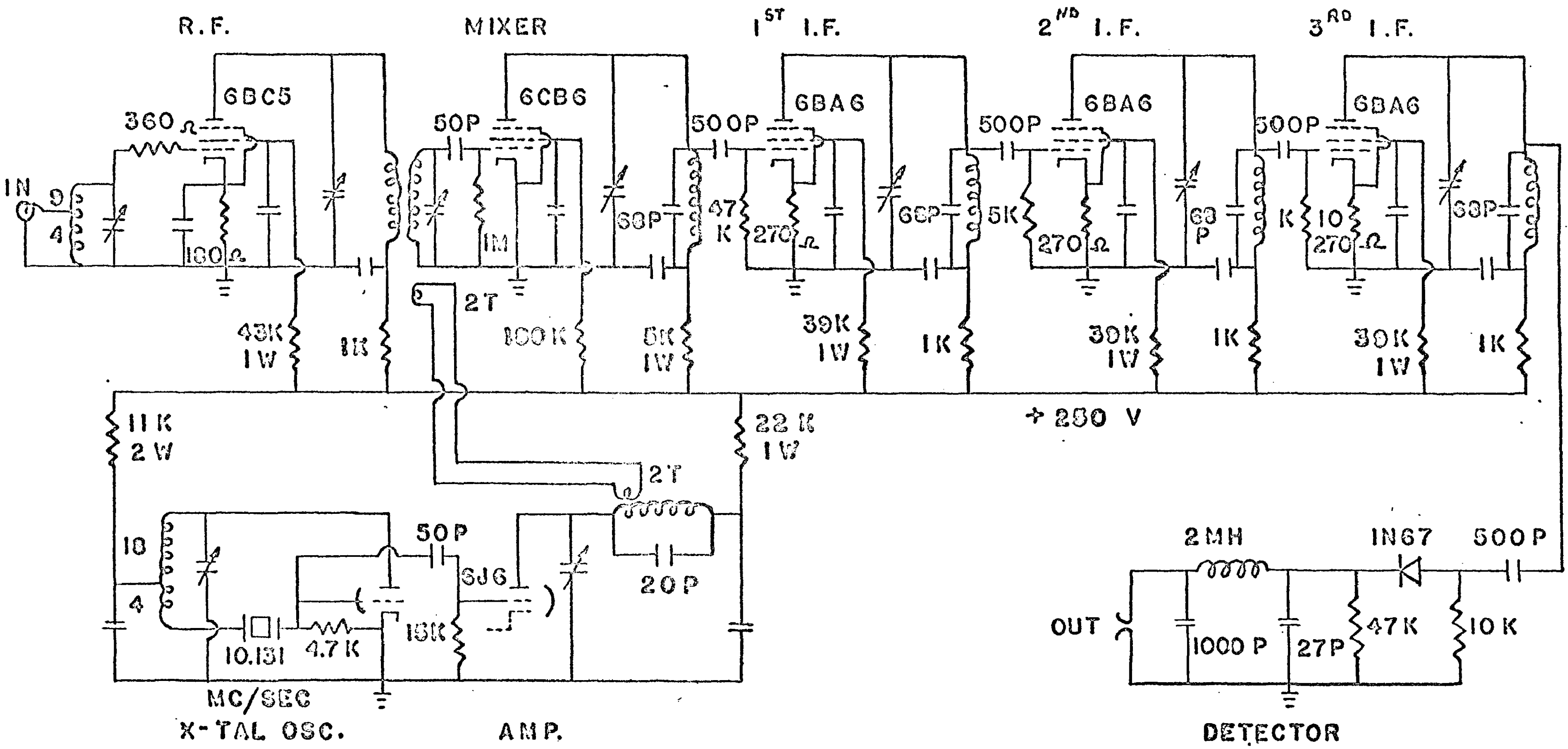

ALL BI-PASS CAP. = 0.005 μF
ALL TUNING CAP. = 3-30 $\mu\mu$F

R.F. COIL	13 T #21	39 MC/S	
OSC. COIL	22 T #27	30.5 MC/S	
AMP. COIL	11 T #24	30.5 MC/S	
R.F. COIL / MIX. COIL	13 T #21	39 MC/S	
I.F. COIL	25 T #27	8.5 MC/S	

39 MC/S RECEIVER

FIGURE 6

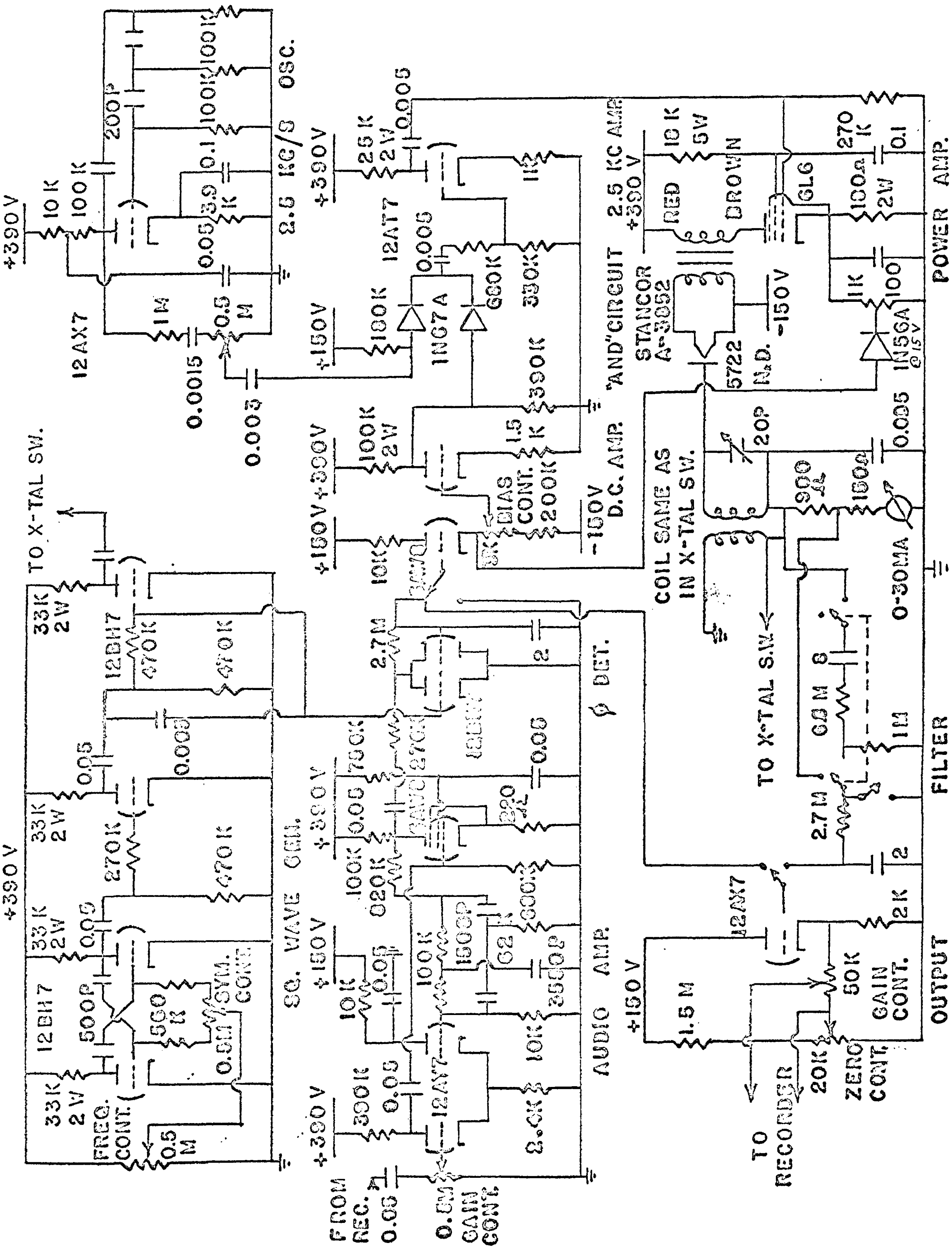
2.5 KC/S OSC.
"AND" CIRCUIT
2.5 KC AMP
D.C. AMP.
POWER AMP.
SQ. WAVE GEN.
φ DET.
FILTER
AUDIO AMP.
OUTPUT
TO X-TAL SW.
TO RECORDER
FROM REC.

FIGURE 7

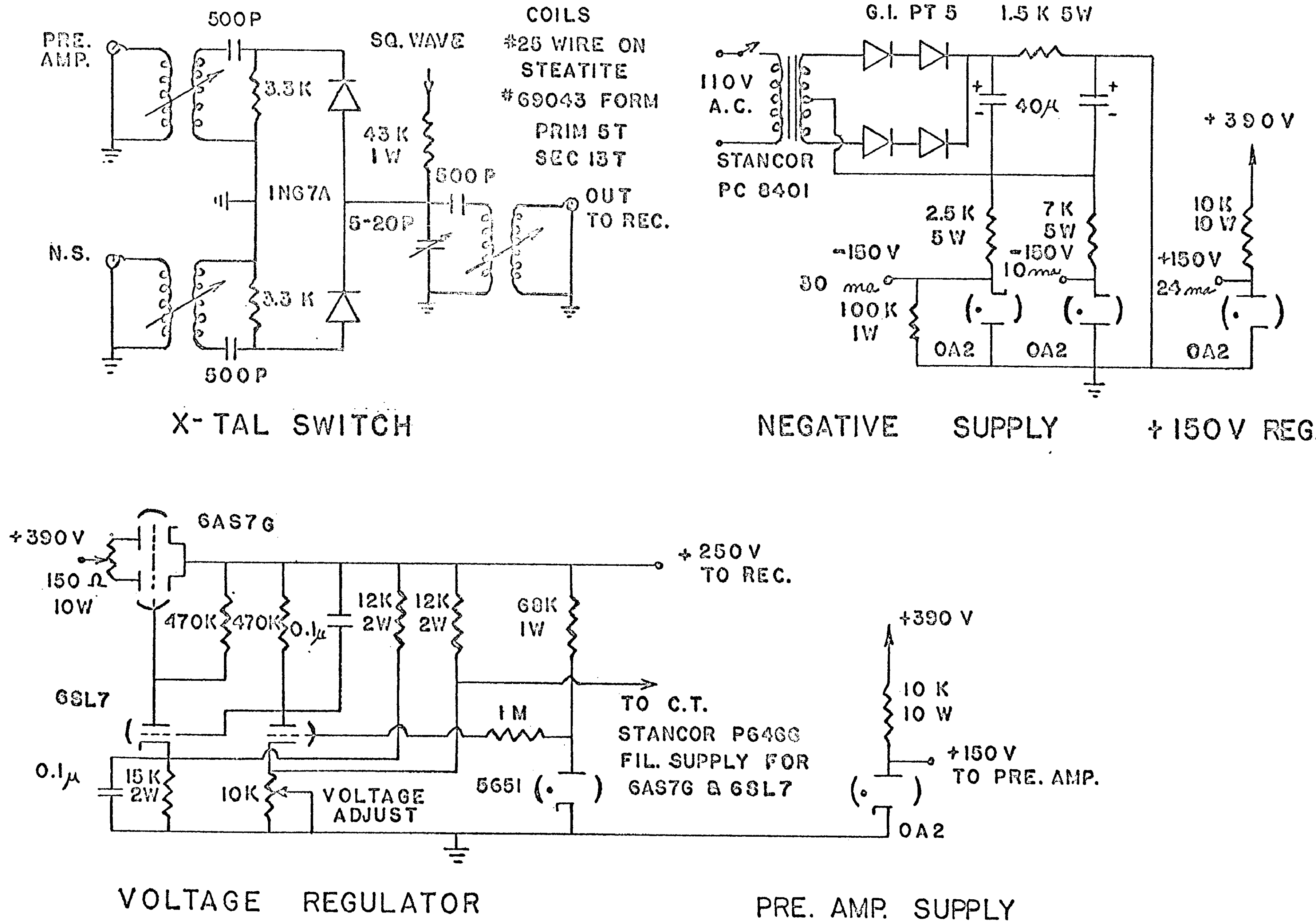
PRE. AMP.
500P
3.3K
SQ. WAVE
COILS
#25 WIRE ON
STEATITE
#69043 FORM
PRIM 5T
SEC 13T
43K
1W
500P
IN67A
5-20P
OUT
TO REC.
N.S.
3.3K
500P
X-TAL SWITCH
G.I. PT 5
1.5K 5W
110V
A.C.
40μ
STANCOR
PC 8401
+390V
2.5K
5W
7K
5W
10K
10W
-150V
30 ma
100K
1W
-150V
10 ma
+150V
24 ma
OA2
OA2
OA2
NEGATIVE SUPPLY
+150V REG.
+390V
6AS7G
150 Ω
10W
+250V
TO REC.
470K
470K
0.1μ
12K
2W
12K
2W
68K
1W
+390V
6SL7
TO C.T.
1M
10K
10W
STANCOR P6466
FIL. SUPPLY FOR
6AS7G & 6SL7
0.1μ
15K
2W
10K
VOLTAGE
ADJUST
5651
+150V
TO PRE. AMP.
OA2
VOLTAGE REGULATOR
PRE. AMP. SUPPLY

FIGURE 8

Satellite Receiving Equipment

A detailed description of the satellite receiving equipment is given by Alexander.[21] For completeness, a general description of the receiving system will be given here.

The antennas used for satellite tracking were half wave folded dipoles tuned to 59 Mc/s. Construction of these antennas is described by Martin.[22] The antennas were aligned so that one was in the north-south direction while the other was aligned in the east-west direction in such a way that their midpoints intersected. The antennas were supported by aluminum masts about 30 feet above the ground thus reducing the effect of ground obstructions. The ground plane was not known, nor was an artificial one constructed.

A Tapetone TC-54 converter was used to convert the 54 Mc/s satellite signal to an intermediate frequency of 14.4 Mc/s. The converter unit incorporates a cascode R.F. amplifier stage and crystal controlled local oscillator. The entire unit has a gain of 44 db and a noise figure of 3.2 db.

The signal from the converter was fed to a Collins 51J-4 radio communications receiver. The receiver is a superheterodyne employing single, double, and triple conversion to tune the frequency range of 540 Kc/s to 30.5 Mc/s in 30 one megacycle bands for AM or CW reception. A setting error and drift of less than 1 Kc/s is attainable with frequency stability within 300 cps at room temperature. The sensitivity is such that less than a five microvolt signal gives a signal to noise ratio of about ten db. For the input frequency of interest (14.4 Mc/s) dual conversion is used. One stage of R.F. amplification is used on all bands. The signal frequency is beat against a crystal controlled high frequency oscillator to produce an intermediate frequency of 1.6 Mc/s. This signal is then combined in the second mixer with the v.f.o. output to produce a 500 Kc/s fixed I.F. The output of the second mixer stage is then amplified by a 500 Kc/s I.F. amplifier. The second intermediate channel is fixed tuned to 500 Kc/s. It consists of a mechanical filter followed by four amplifier stages. The output of the second intermediate channel is then fed to the detector. The detector is one half of a 12AX7 dual triode tube used as a diode with rectification taking place between the plate and the cathode, the grid being connected to the plate. The output signal is taken from the diode test point above a 100 K load resistance in parallel with a 330 $\mu\mu$ farad capacitor for R.F. filtering. The signal is then fed to a cathode follower to present a constant impedance to the detector after which it is integrated to prevent amplification of frequencies higher than the linear response of the recording system. The output of the integrator is fed to a four channel Brush Pen Recording System (Model RD 5211-03) which provides sensitivity in steps of 0.01, 0.02, 0.05, 0.1, 0.2, 0.5, 1, 2, 5, and 10 volts per chart line (mm). This range permits full scale measurements from 0.04 to 400 volts. The pen motor has a d.c. sensitivity of 1.5 volts per mm. The frequency response is such that the recorded peak to peak amplitude of a constant voltage sine wave will be within $\pm$ 1/2 chart line of nominal 40 lines from d.c. to 10 cps or within $\pm$ 1 chart line of a nominal 10 lines from d.c. to 100 cps. Measured trace linearity is with two percent of full chart width at any frequency up to 100 cps. The maximum amplitude is 40 lines peak to peak up to 40 cps, 20 lines up to 70 cps and 10 lines up to 100 cps. An eight speed transmission provides chart speeds of 1, 2, 5, 25, 50, 125, and 250 mm per second.

A Model SR-7 receiver was used to record WWV transmissions. It is of the fixed frequency type utilizing crystal control for frequency selection.

A block diagram of the system is shown in Figure 9.

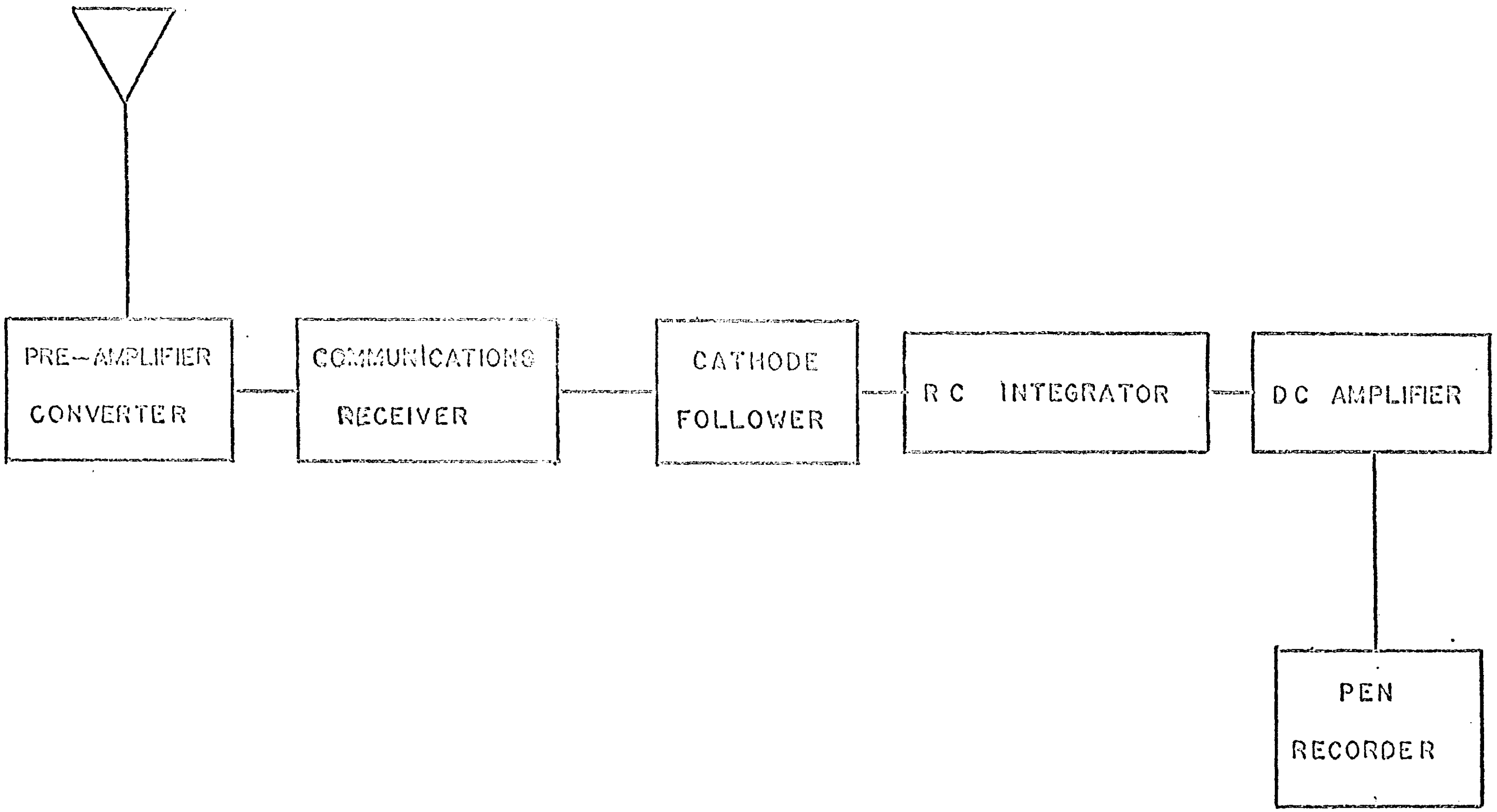

BLOCK DIAGRAM OF RECEIVING EQUIPMENT

FIGURE 9

EXPERIMENTAL PROCEDURE

Using the equipment described in the preceding section simultaneous star observation and satellite passes were recorded during the period July 1963 through August 1963. Several previous simultaneous observations have been included in this study and are listed in Table 3.

Satellite arrivals were computed using prediction bulletins supplied by Goddard Space Flight Center. Position computations of the radio source Cassiopeia A are described in detail by Hollinger. Forty-six useable simultaneous star and satellite passes have been analyzed for scintillation.

Method of Analysis of Star Data

The output of the star receiving equipment was recorded on a fixed span G-10 Varian recorder. The chart paper is five inches wide with subdivisions of one twentieth of an inch, each corresponding to one millivolt deflection. The balance position was chosen at 40 millivolts, and all recordings were made with a chart speed of one inch per minute. Gradual, prolonged fluctuations were eliminated by and band pass filter incorporated in the system. The star remained in the 45° beamwidth of the antenna for about three hours. Recordings were taken so that the half-hour satellite records spanned the middle of the three hour star records, rendering maximum reception of the star signal during the satellite pass.

The star records were analyzed for this half-hour period by visual comparison with a set of preanalyzed records. Six minute intervals of the star recordings were compared to equal intervals of records whose fluctuation indices were computed by measuring the amplitude of the signal at 15 second intervals. The indices for these six minute intervals were then averaged over the total half-hour pass giving rise to an average fluctuation index for the pass. The fluctuation index is defined here as the ratio of the root mean square deviation from the mean to the mean amplitude:

$$F.I. = \frac{\sqrt{\frac{\Sigma (X_i - \overline{X})^2}{N}}}{\overline{X}}$$

where X_i is the i^{th} signal amplitude, $\overline{X}$ the mean value, and N the number of measurements.

Background noise gives rise to an index of about 0.025, while 0.032 is characteristic of weak scintillation. An index of 0.260 is indicative of strong scintillation. Six minute intervals of sample records are shown in Figure 10 . Record A shows no scintillation and is equivalent to background noise. Records B and C have indices of 0.032 and 0.107 respectively. Record B illustrates weak scintillation while C is characteristic of moderate scintillation. Records D and E have indices of 0.225 and 0.260 respectively and indicate strong scintillation.

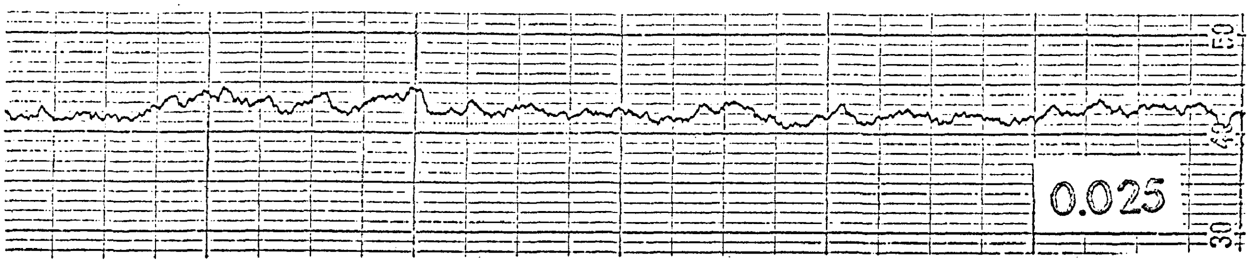

A

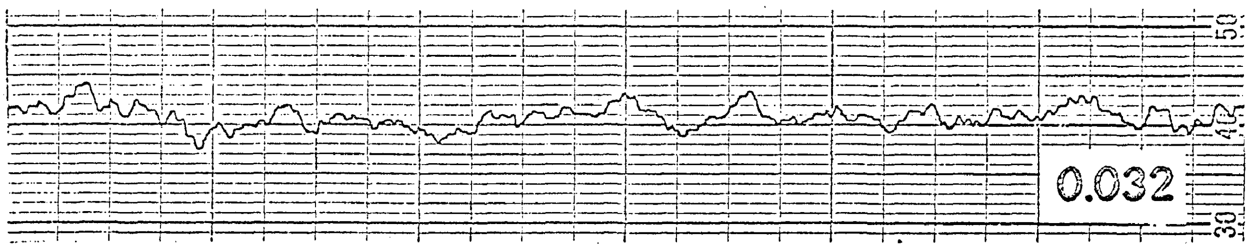

B

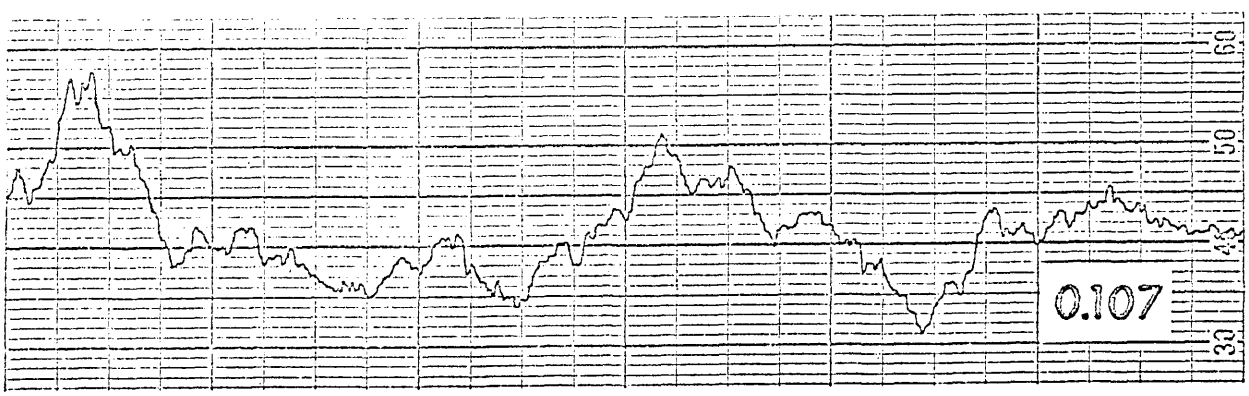

C

EXAMPLES OF STAR FLUCTUATION INDICES

FIGURE 10

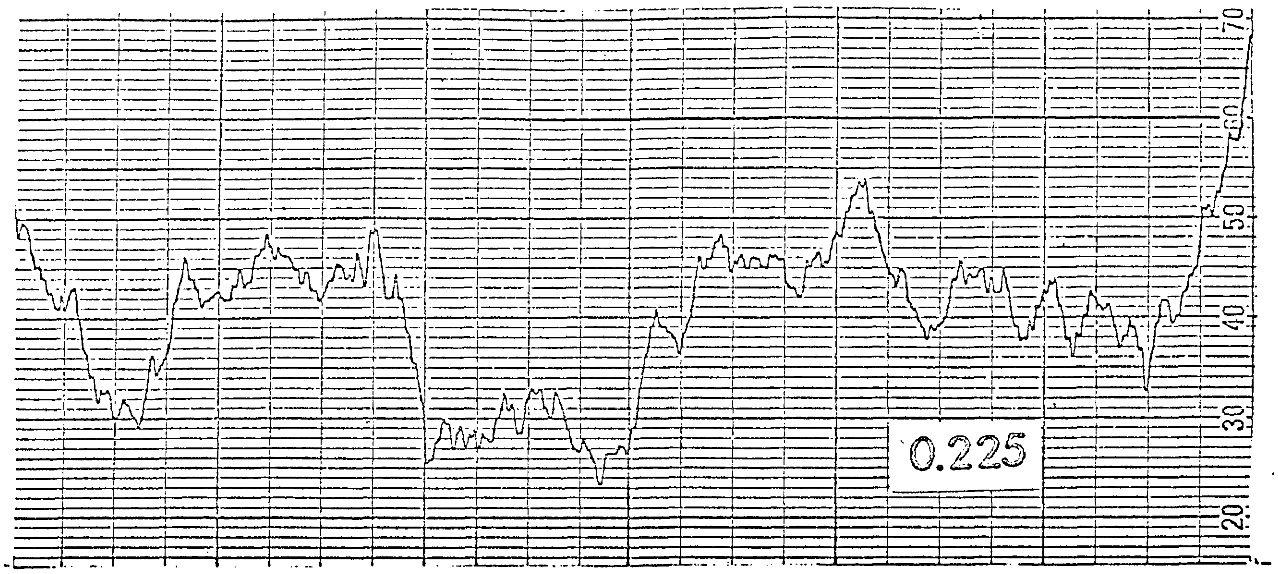

D

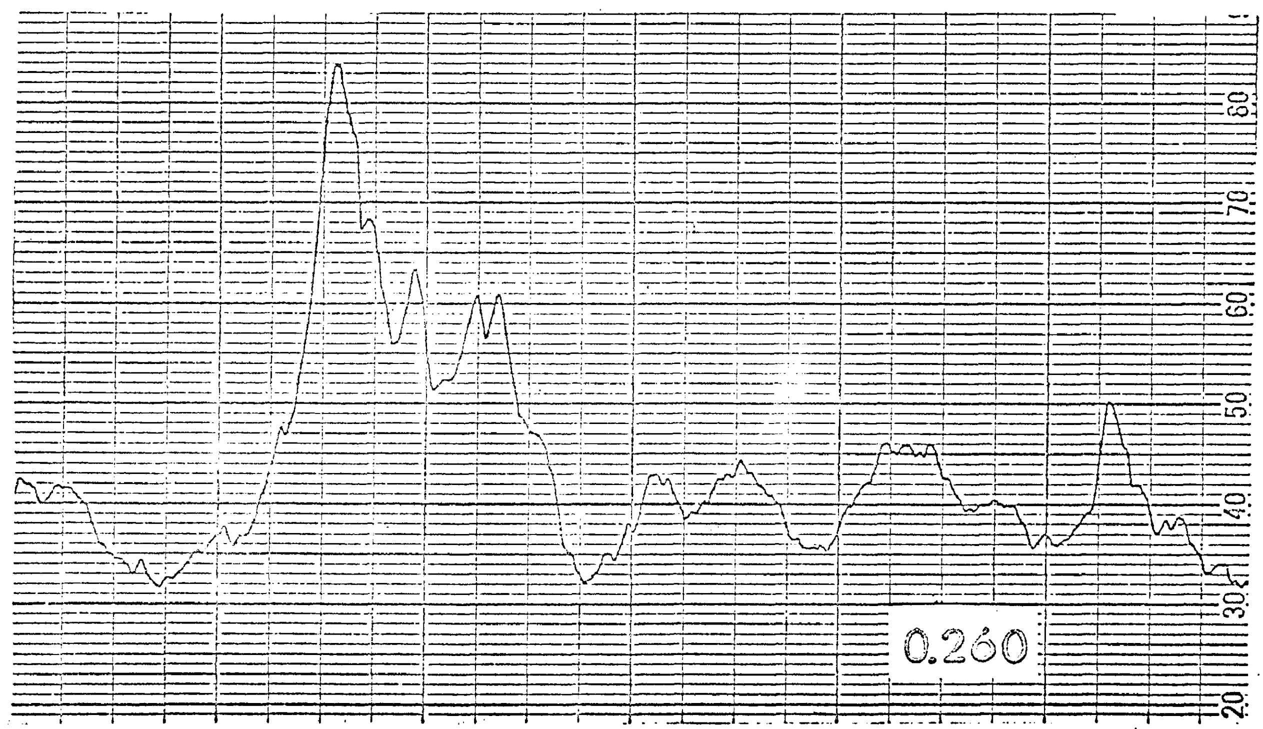

E

FIGURE 10 CONTINUED

Method of Analysis of Satellite Data

Because of the rapid fading rate of satellite scintillation, computation of the scintillation index as described in the previous section is impractical. Consequently a scintillation index was assigned by visual inspection to every ten second interval of the satellite record as a measure of the scintillation depth. The indices for ten second intervals were averaged over the entire half-hour record giving rise to an average scintillation index for each pass. The indices used are modifications of those proposed by Yeh and Swenson and are shown in Table 2.

TABLE 2

0.0	Record exhibits only regular fading due to Faraday rotation and rotation of the satellite.
0.5	Record exhibits conditions described by 0.0 but has superimposed irregular fading whose amplitude is less than 50% of the maximum signal strength.
1.0	Record exhibits condition described by 0.0 but has superimposed severe irregular fading whose amplitude is greater than 50% of the maximum signal strength.
1.5	Signal is weak and irregular, but bursts of regular fading are noted. No Faraday rotation is evident. The satellite is generally at low elevation angles.
2.0	Signal is very strong, but all evidence of regular fading is completely obscured. The fluctuations have large amplitudes and usually occur at a rapid rate.

Figure 11 shows two samples of each index.

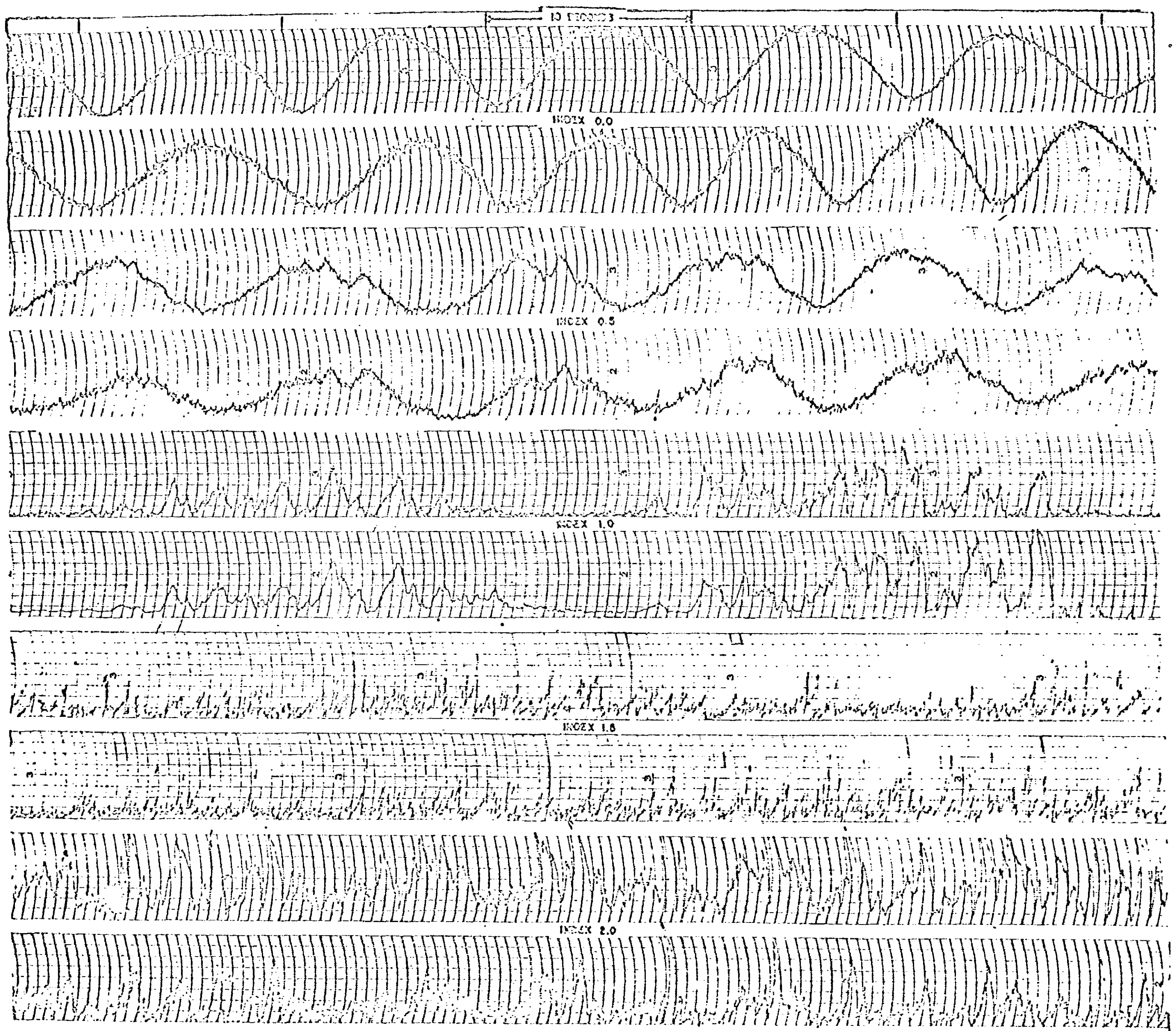

FIGURE 11 SCINTILLATION INDICES -- TRANSIT IV-A

EXPERIMENTAL RESULTS

A linear correlation analysis was done on 46 simultaneous star and satellite passes. In Figure 12 the average fluctuation index of the star signal is plotted as a function of the average scintillation index of the satellite signal. A summary of the data is given in Table 3. The coefficient of correlation between these two sets of data is -0.18. The significance level of the correlation coefficient for 46 data elements is .25 . These results seem to indicate that there is no linear relationship between star and satellite scintillation. This might be anticipated due to the random nature of the scintillation. Satellite records illustrate rapid variation from periods of weak scintillation, while radio star scintillation is thought to be constant over large areas (400 miles) and over periods of time of several hours.[33] This effect is generally attributed to the large velocity difference of the sources. These results are in general agreement with those of Slee,[8] Parthasarathy and Reid,[9] and Lawrence.[23]

Assuming the density distribution of the irregularities in the area of the sky over the receiving station to be constant, no attempt was made to observe the satellite and star simultaneously in the same part of the sky. Also these data were taken at sunspot minimum. Briggs[16] has shown that radio star scintillation is a minimum at this time. Another fact accounting for the generally low values of star scintillation indices is that during the period of observation (summer 1963) Cassiopeia A appeared

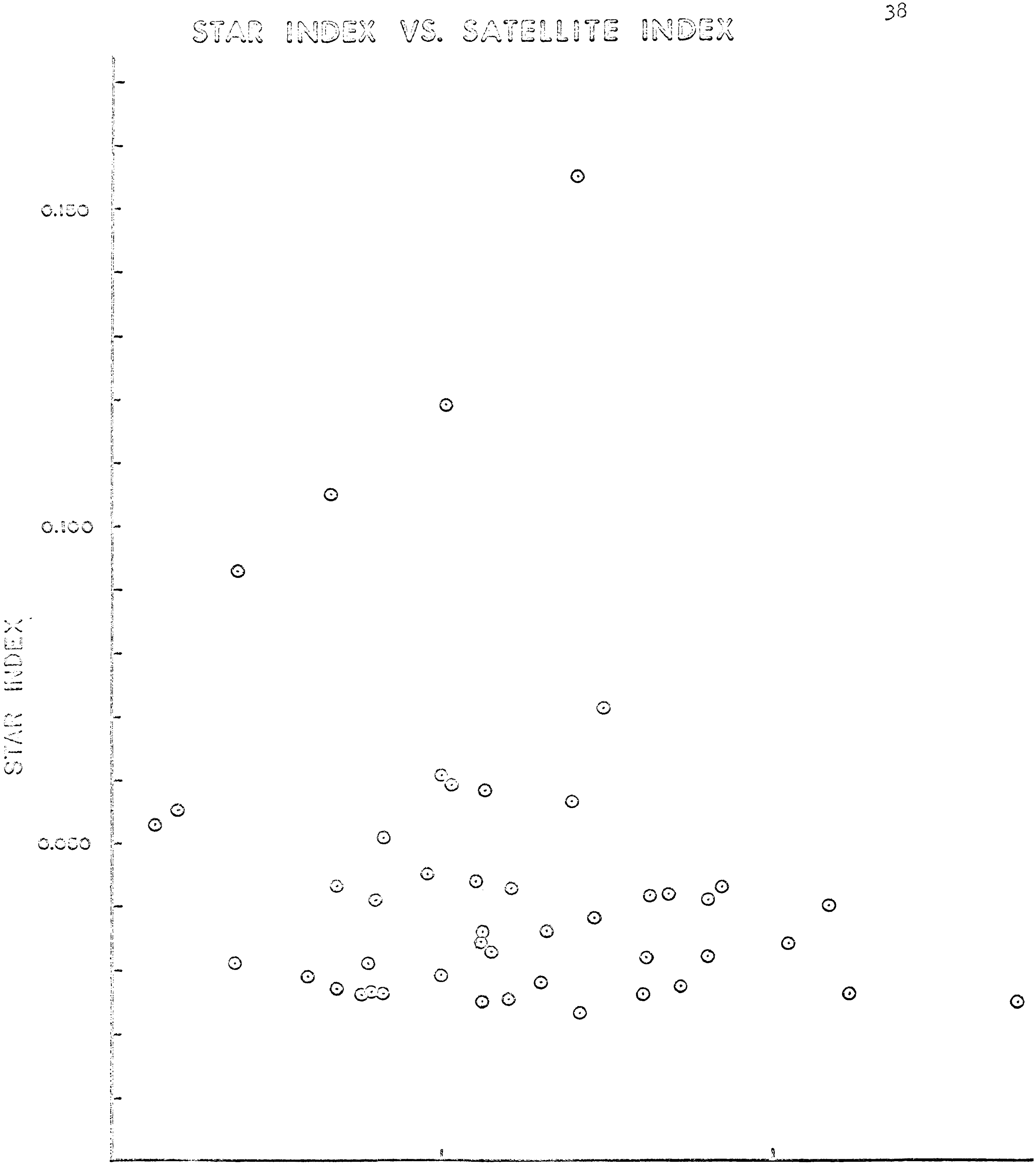
STAR INDEX VS. SATELLITE INDEX
0.150
0.100
0.050
STAR INDEX
0.5
1.0
SATELLITE INDEX

FIGURE 12

TABLE 3

Record Number	Time E.S.T.	Data	Fluctuation Index of Star	Av. Index of Satellite
1	2310	2-11-62	0.060	0.50
2	1107	3-20-62	0.093	0.19
3	1152	4-17-62	0.155	0.70
4	1448	4-30-62	0.029	0.50
5	0750	7-19-62	0.034	0.56
6	1124	7-19-62	0.029	0.30
7	2244	7-19-62	0.246	0.82
8	0830	7-29-62	0.032	0.57
9	0814	7-30-62	0.034	0.56
10	1800	11-12-62	0.026	0.80
11	2020	4-16-63	0.025	0.60
12	2132	7-4 -63	0.026	1.11
13	2318	7-4-63	0.032	0.90
14	1241	7-5 -63	0.023	0.71
15	1427	7-5 -63	0.105	0.33
16	2147	7-5 -63	0.027	0.86
17	2333	7-5 -63	0.025	0.56
18	2216	7-7 -63	0.040	1.18
19	1152	7-9 -63	0.043	0.60
20	1336	7-9 -63	0.041	0.40
21	2057	7-9 -63	0.025	1.37
22	2244	7-9 -63	0.041	0.90
23	1207	7-10-63	0.056	0.69

TABLE 3 (Continued)

Record Number	Time E.S.T.	Date	Fluctuation Index of Star	Av. Index of Satellite
24	1350	7-10-63	0.043	0.34
25	1207	7-11-63	0.028	0.65
26	2313	7-12-63	0.027	0.34
27	1235	7-12-63	0.044	0.55
28	1830	7-21-63	0.043	0.92
29	1845	7-22-63	0.034	1.02
30	0131	7-23-63	0.055	0.10
31	1322	8-13-63	0.032	0.81
32	1351	8-15-63	0.045	0.48
33	1218	8-16-63	0.071	0.74
34	1114	8-19-63	0.042	0.84
35	1301	8-19-63	0.028	0.65
36	1205	8-21-63	0.059	0.51
37	1158	8-22-63	0.026	0.40
38	1343	8-22-63	0.036	0.56
39	1254	8-26-63	0.119	0.50
40	0937	8-27-63	0.038	0.73
41	1124	8-27-63	0.051	0.41
42	0952	8-28-63	0.058	0.56
43	1137	8-28-63	0.036	0.66
44	1006	8-29-63	0.026	0.38
45	1152	8-29-63	0.031	0.19
46	1020	8-30-63	0.031	0.39

only at high elevation angles. It has been shown[16] that the scintillation index decreases with increasing elevation angles, tending to a minimum at high elevation angles. Consequently, it is difficult to observe even a general correlation between star and satellite scintillation indices as was observed by Slee. Of the 46 passes taken, on 28 nights of 41 when the star scintillation index was low, the satellite scintillation index was low. Of the 5 nights when the star scintillation index was high, there were 3 nights when the satellite scintillation index was high. Due to the lack of sufficient scintillation activity in the radio star signal a general correspondence cannot be inferred.

In order to further investigate the possibility of a general correlation between star and satellite amplitude scintillation a detailed comparison of satellite studies made at the College of William and Mary and published features of star scintillation will be made.

Briggs[16] has conducted the most comprehensive and extensive investigation of radio star scintillation to date. Cassiopeia A was observed at a frequency of 38 Mc/s at Cambridge (52° N, 0° E) over the period 1949 to 1961. During this time, Briggs observed a distinct variation of the scintillation index with the solar cycle. The scintillation index has its largest value at sunspot maximum (1957 - 1958) and a minimum value at sunspot minimum (1954 - 1955). Chivers,[24] observing the signal of Cassiopeia A over a period of four years at Jodrell Bank, has noted a similar variation with the sunspot cycle. Both observers have noted a negative correlation between spread F phenomena and radio star scintillation activity over the solar cycle. Booker[5] observed good positive correlation between these two phenomena. His data, however, do not extend over a complete solar cycle. It is generally agreed[25,16] that spread F and radio star scintillation are night time phenomena. Dagg,[26] at Jodrell Bank, has conducted a study of radio star scintillation and spread F over the period 1954 to 1955. He observed a marked correlation between fluctuation and spread F although this correlation was not found to exist on an hour to hour basis. The diurnal maximum of occurrence of scintillation was found to be several hours earlier than that of spread F. There is also a seasonal variation of spread F which is not apparent in the observation of radio star scintillation.

All observers agree[5] that there is a maximum of amplitude scintillation in the middle of the night. Using four sources, Ryle and Hewish[27] have plotted the fluctuation index as a function of time shown in Figure 13, where a midnight maximum is clearly evident. Briggs has eliminated variations with solar time by successively averaging 12 monthly mean curves of fluctuation index versus GMT for each sidereal hour, introducing successive displacements of two hours. This averaging process leaves only the variations with sidereal time. All curves averaged in this manner exhibit maxima near midnight and are fairly symmetrical about these maxima. Little and Maxwell,[28] at Manchester, observed that the fluctuations are largest at night. The note, however, that at low elevation angles, fluctuations appear to be independent of the hour of the day; a similar observation was made by Bolton, Slee, and Stanley[29] in Australia. Bolton et al. observe, in addition to a midnight maximum, a maximum at midday of comparable importance as shown in Figure 14. Harrower[30] has made a study of diurnal and seasonal variation in the occurrence of amplitude scintillation at Ottawa. His results are given in Figure 15. By averaging a year's data, the dependence of zenith angle upon the occurrence of amplitude

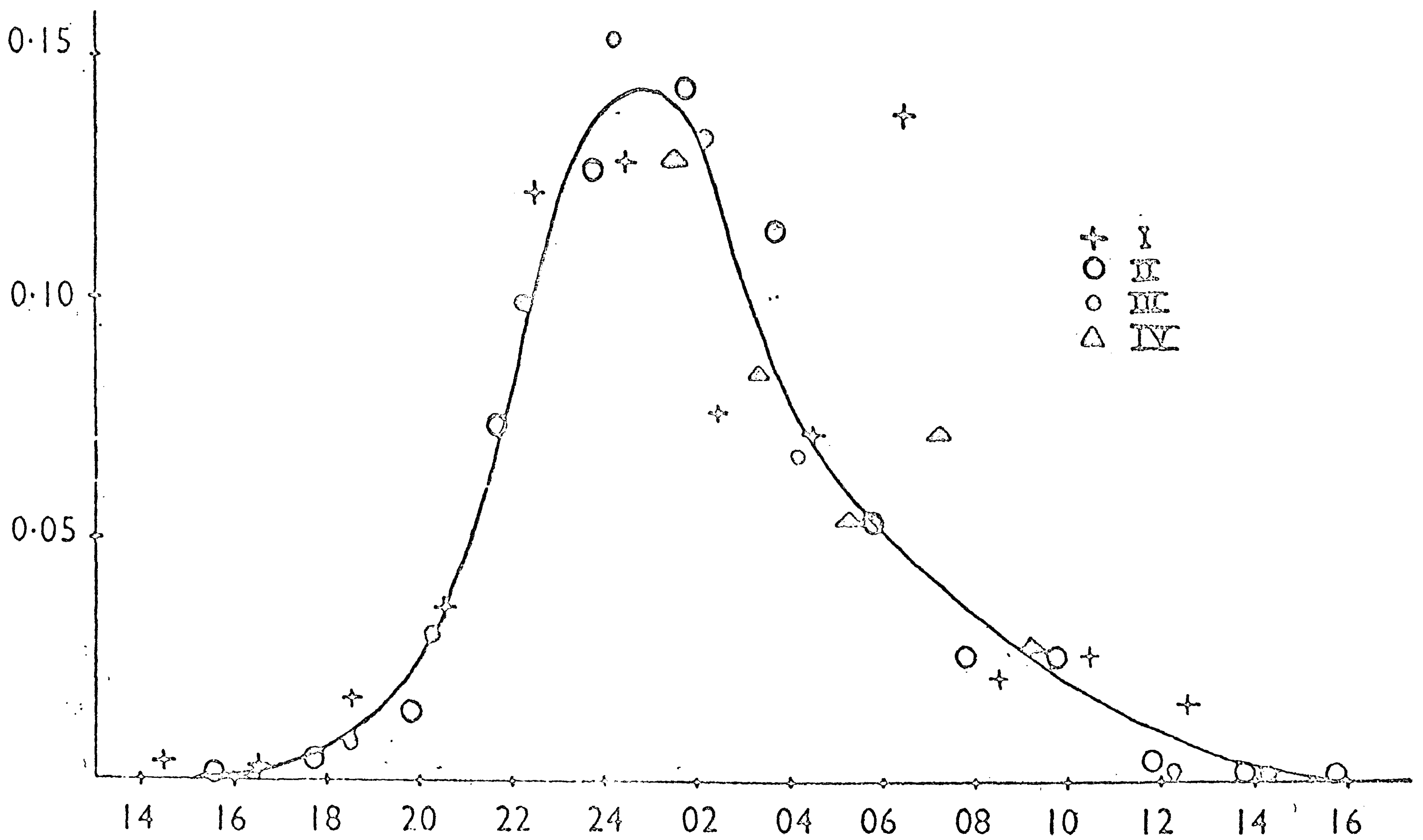

Variation of the "fluctuation index" for the four sources plotted as a function of the time of observation. Ordinates: Fluctuation index. Abscissae: Local time.

FIGURE 13 (Ryle and Hewish)

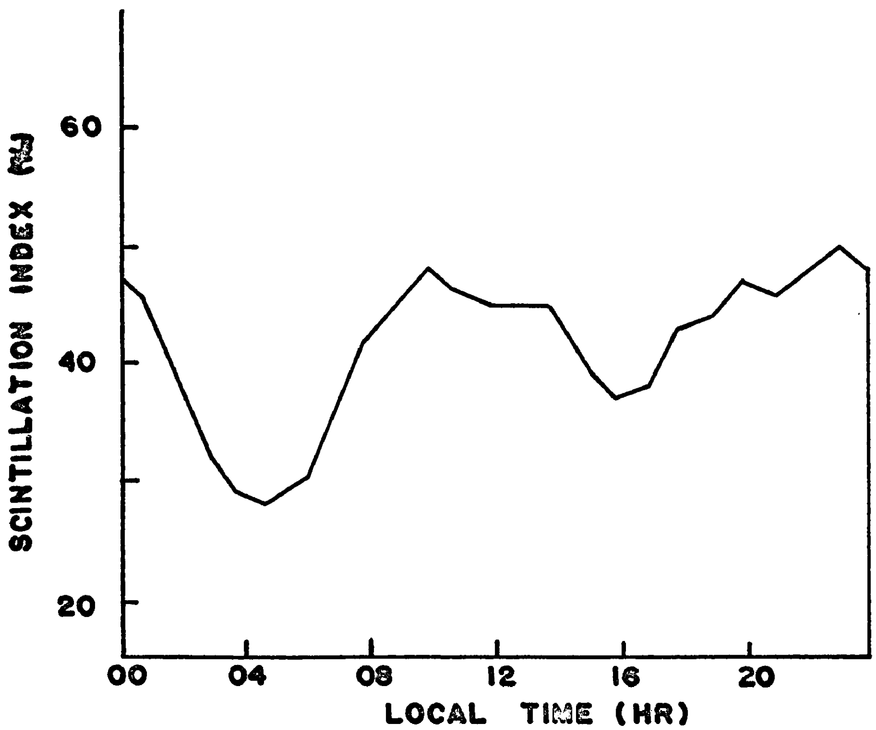

MEAN MONTHLY SCINTILLATION INDEX VS. LOCAL TIME OF OBSERVATION

(Bolton, Slee, and Stanley)

FIGURE 14

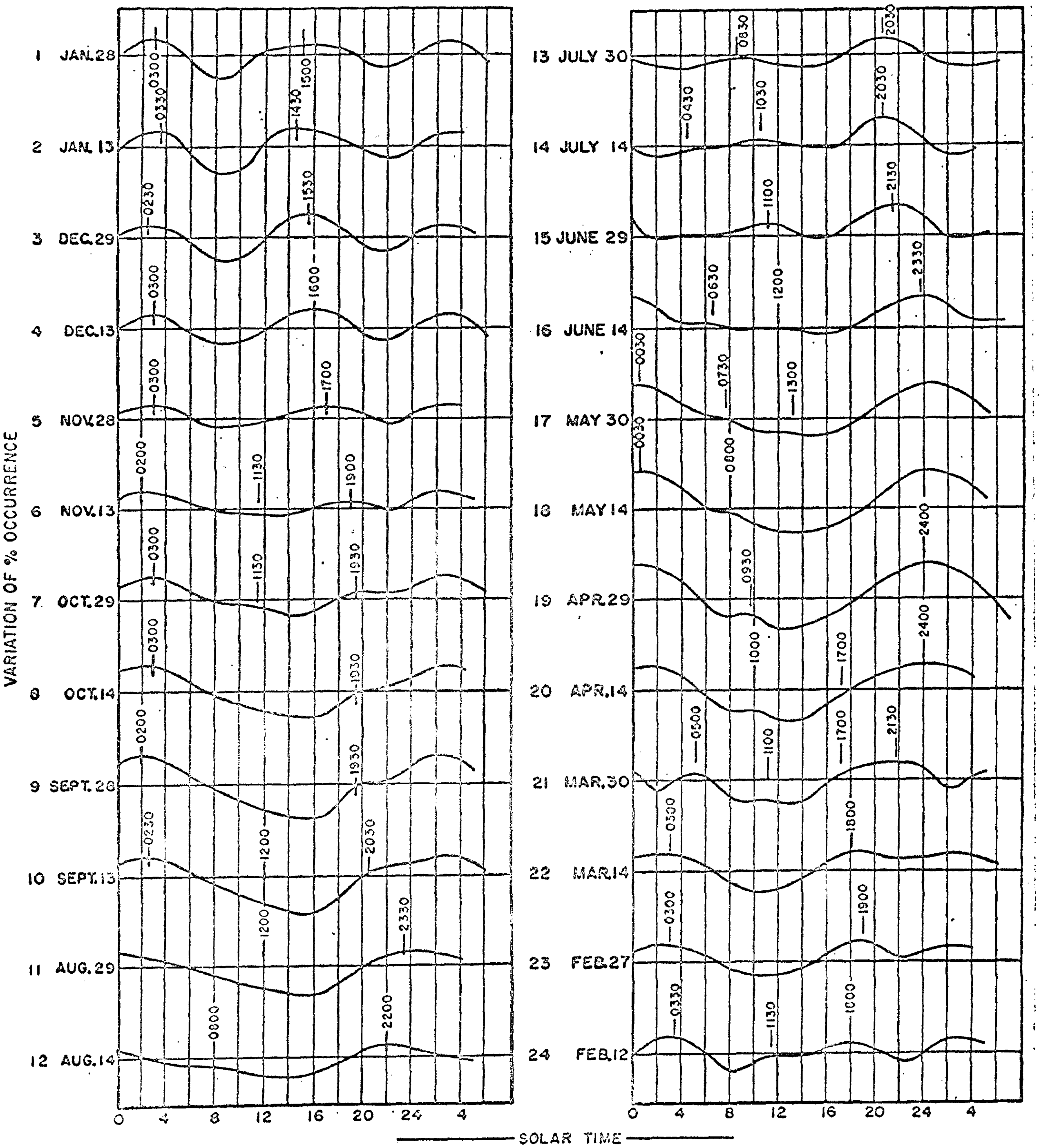

Each of the 24 graphs shows variation of the percentage occurrence of scintillations plotted against local mean solar time for a given 15-day interval centered about the date written beside the graph. The numbers from 1 to 24 are used to identify 24 positions of the earth on its orbit around the sun in the course of one year. The hours marked along the curves indicate the times during the day at which the occurrence of scintillations passed through a maximum.

FIGURE 15
(Harrower)

scintillation was found. By means of this curve, all data were converted into zenith observations. This corrected data then gave the diurnal and seasonal variations illustrated in the figure. This curve also illustrates a night time maximum in the rate of occurrence throughout the year. There is also a daytime maximum in the winter and a smaller daytime maximum in the summer. Their observations generally agree with those of Bolton, et al. It may be concluded, then, that amplitude scintillation is definitely a night time phenomena at all but low elevation angles, with a maximum near midnight. In addition, some observations indicate the presence of a weak midday maximum.

Briggs has examined variations of the fluctuations index with the hour angle of the source over the period 1949 to 1961. His curves show a maximum at the time of lower transit and fall off symmetrically about this maximum. Chivers, during the period 1955 to 1958, made a similar analysis and found that the maximum value of the scintillation index occurred one hour before the time of lower transit. Briggs' curves also show a similar small displacement for these years; however, he concludes that since the displacement is very small and does not appear on all of his curves, it is of doubtful significance.

Briggs has also interpreted these curves as showing the variation of scintillation index with zenith angle, since the zenith angle of the source is a function of the hour angle. Any given zenith angle will occur for two different hour angles. Since the curves of fluctuation index versus hour angle are approximately symmetrical it is permissible to average the two values of the fluctuation index, which are approximately equal, to obtain a mean zenith angle curve. These curves show a continuous increase of scintillation index with increasing zenith angle for the entire period over which data were taken. Booker, at Cambridge and Manchester, has also observed similar zenith angle dependence. (Figure 16). All observers generally agree that there is a marked increase of amplitude scintillation with increase of zenith angle[3].

Briggs and Parkin[31] have conducted a significance study of zenith angle ratios, defined as the ratio of the mean scintillation index at lower transit to the mean scintillation index at upper transit. They have shown that these ratios are larger than can be explained theoretically on the basis of the changing zenith angle alone. As a result of this study, Briggs[16] concludes that the degree of irregularity of the ionosphere must increase with increasing latitude.

In Australia, Bolton et al. have observed a seasonal variation in fluctuation index comparable in importance with the diurnal variation. They observe a minimum at the equinoxes and a maximum at the solstices. Chivers, however, observed an opposite variation, the maximum activity occuring at the equinoxes and a minimum of activity occuring at the solstices. Briggs concludes that his results give no support to the suggestion that the scintillation effect is a maximum at the equinoxes; moreover, it is concluded that if there is any seasonal variation it must be very small. This is also in agreement with the results of Dagg.

A description of satellite studies conducted at the College of William and Mary is given by Lawrence and Martin[7]. The diurnal variation of satellite scintillation was examined by averaging 509 passes of Transit 4 A over one hour intervals for an entire 24-hour day. Data

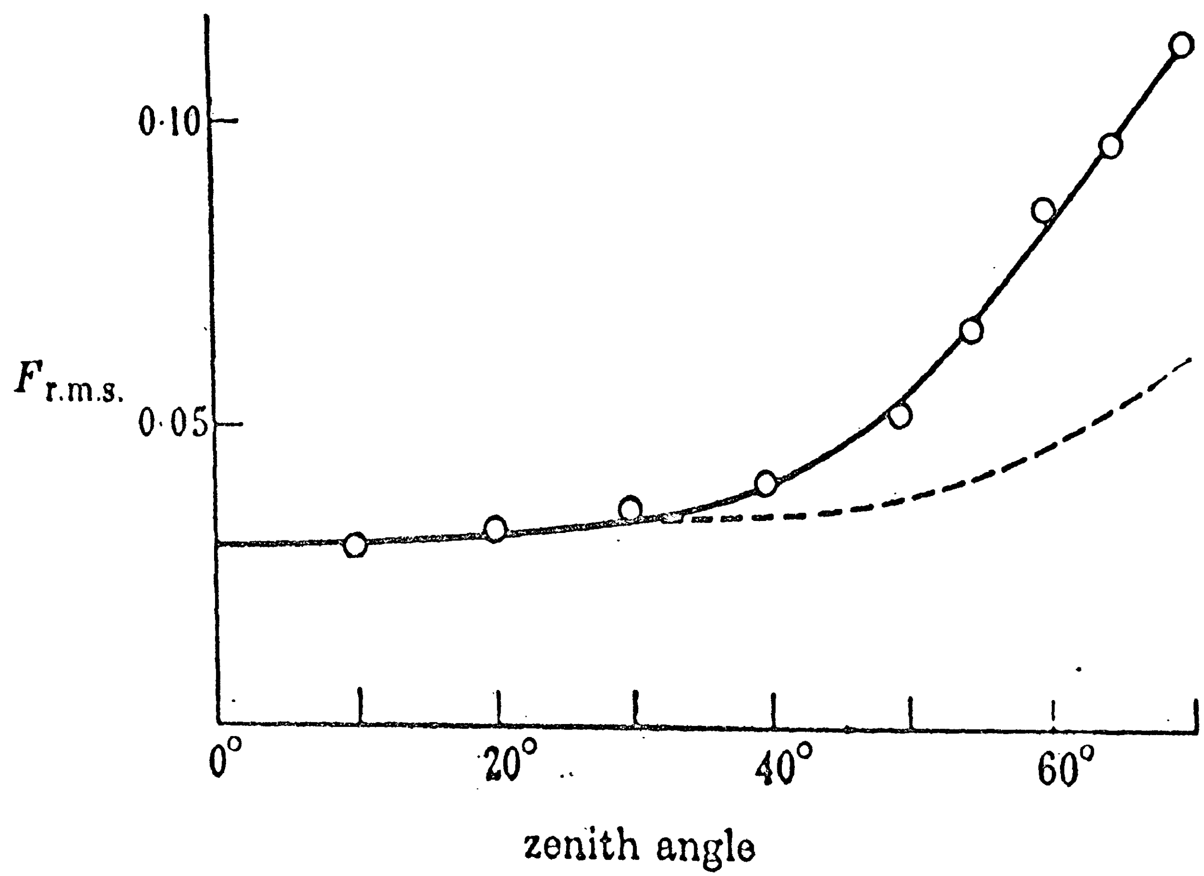

The dependence of the fluctuation index (F_{rms}) upon the zenith angle of the source. The secant of the angle of incidence on the ionosphere at a height of 400 km is shown by the dotted curve.

FIGURE 16
(Booker)

for this study were taken for the period January 1962 through February 1963. Figure 17A shows this hourly average for all months of the year and for all elevation angles. A distinct maximum is evident shortly after midnight. A similar midnight maximum is reported by all observers for radio star scintillation. Figure 17A also shows a secondary maximum occurring at midday. Bolton, Slee and Stanley in Australia observe a similar midday maximum for radio star scintillation as does Harrower in Canada. This secondary maximum is not observed in the United States or in England. To examine the elevation effects on the diurnal study, the data were reaveraged for elevation angles above and below 20°. The resulting curves are shown in Figures 17B and 17C respectively. The midday maximum is still evident for elevation angles less than 20°, but is not as evident for elevation angles greater than 20°. The midnight maximum is still apparent on both curves.

To investigate the variation of satellite scintillation with latitude, the average scintillation index was plotted as a function of latitude for each hour of the day for elevation angles greater than 20°. The resulting histograms are shown in Figure 18. These histograms show that during periods of relatively strong scintillation, there is a distinct variation of the scintillation index with latitude. During these periods scintillation activity appears to be a minimum at the latitude of the observation station (37° N) and increases when the satellite moves to the north or south of the station. In Figure 19 scintillation indices have been reaveraged over all hours of the day and are plotted as a function of latitude. This curve shows a

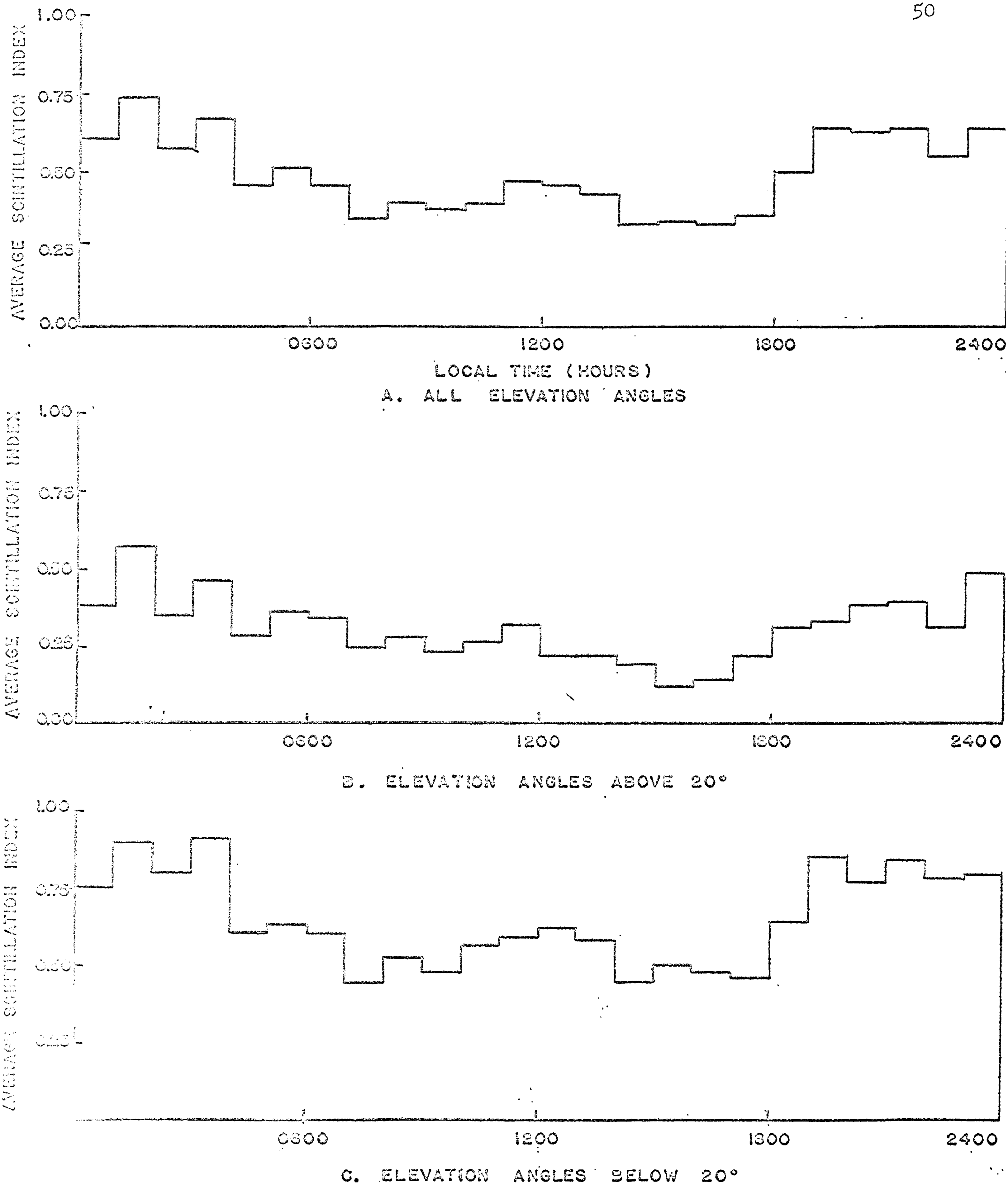

FIGURE 17 AVERAGE SCINTILLATION INDEX VERSUS TIME
(Lawrence and Martin)

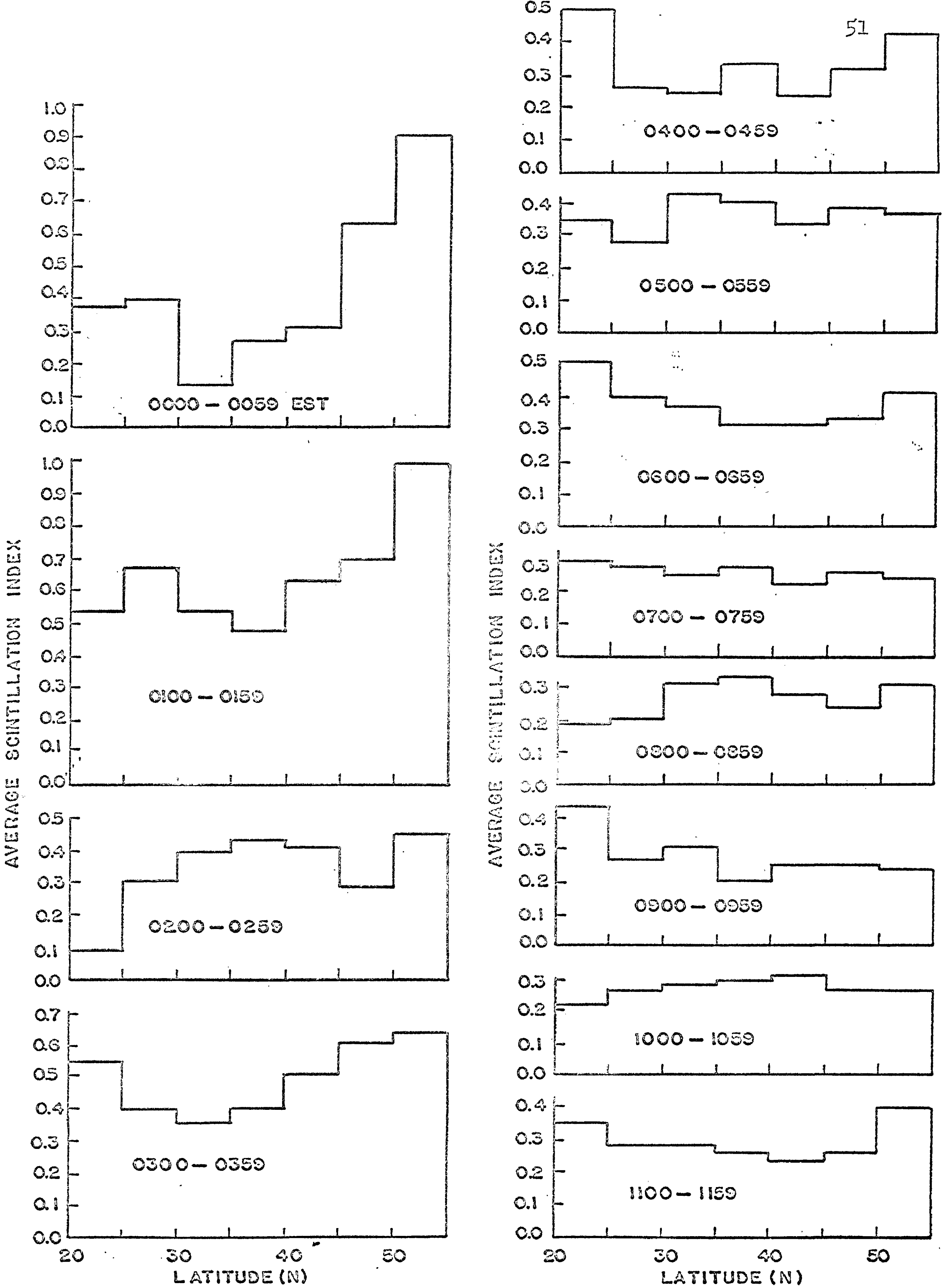

FIGURE 18 DIURNAL VARIATION OF LATITUDE EFFECT

(ELEVATION ANGLES ABOVE 20°)
(Lawrence and Martin)

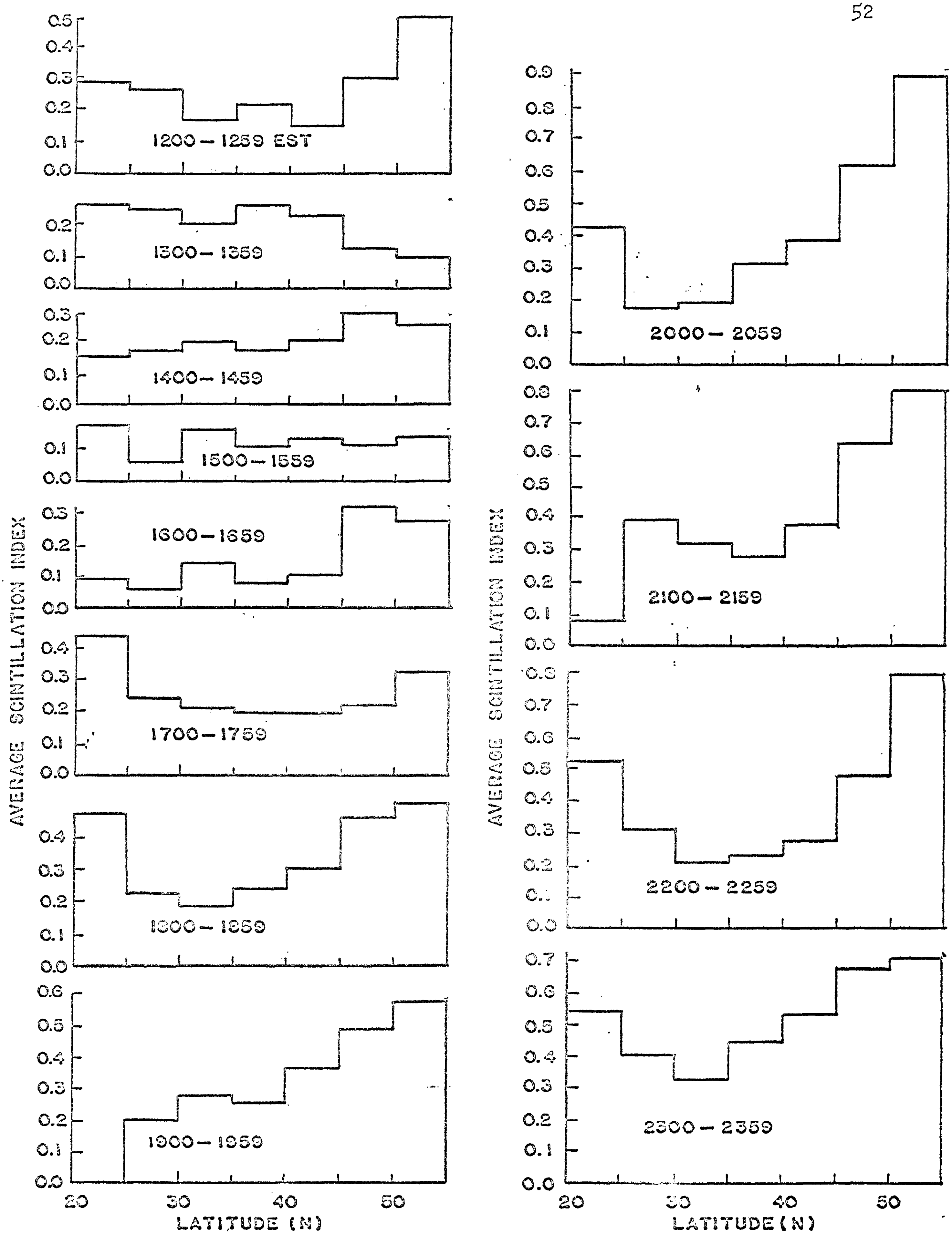

FIGURE 13 CONTINUED DIURNAL VARIATION OF LATITUDE EFFECT

(ELEVATION ANGLES ABOVE 20°)

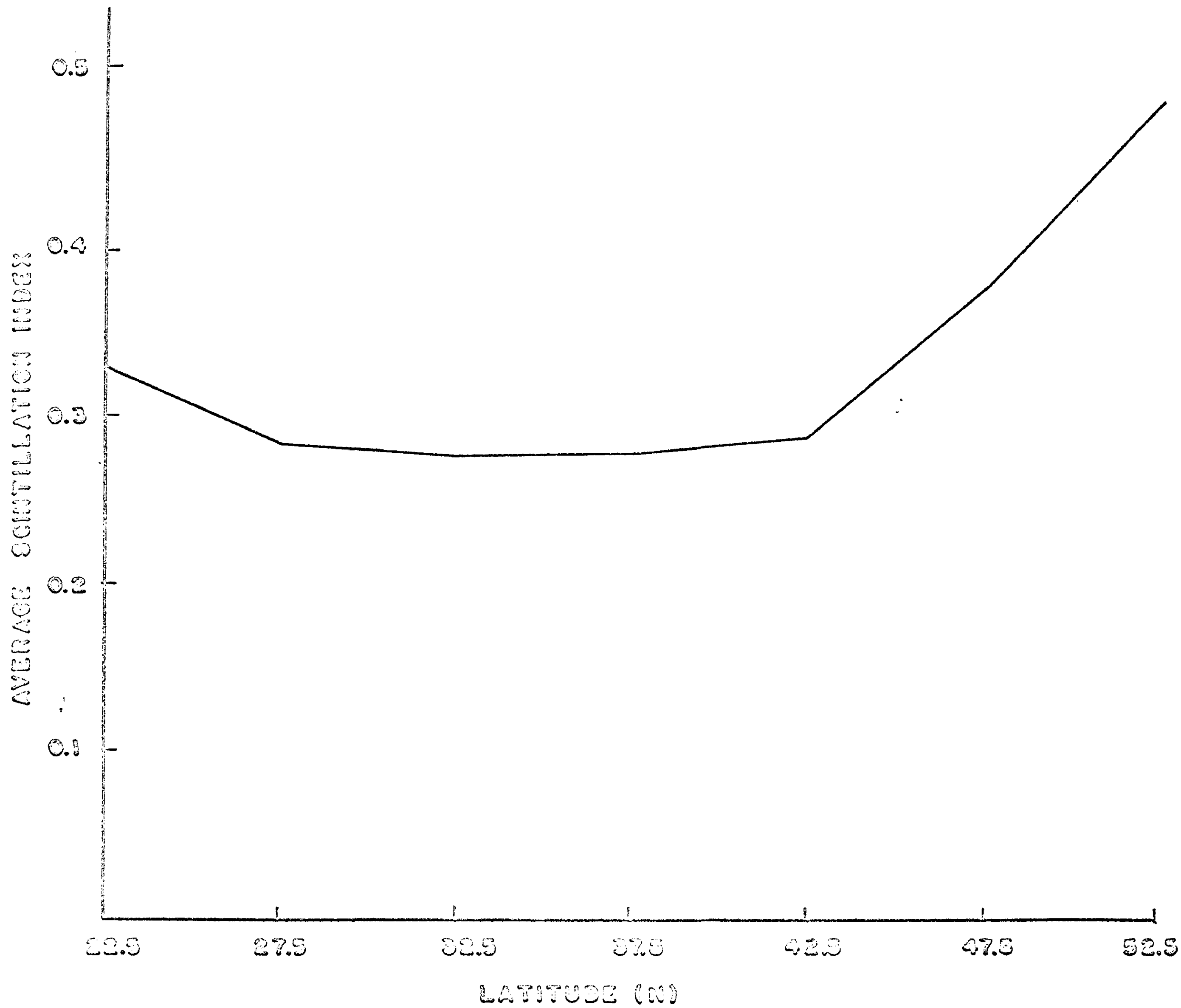

AVERAGE SCINTILLATION INDEX VS. LATITUDE FOR ELEVATION ANGLES ABOVE 20°

FIGURE 19

minimum of activity about 33° latitude. It is interesting to note that the increase of scintillation activity for satellite positions north of the observation station is markedly greater than the increase for positions to the south of the station. Briggs has observed that the scintillation activity for cosmic sources also appears to have a marked latitude effect with greater activity at higher latitudes.

A significance study has been done on the data presented in Figure 18. With reference to Figure 18 this study may be explained as follows: The average scintillation indices for the latitude intervals 20-25, 25-30,...., 50-55 were assigned to latitudes of 22.5, 27.5,...., 52.5 which are the midpoints of the sucessive intervals. This was done for each hour of the day. Thus for each latitude 22.5, 27.5,...., 52.5 there correspond 24 values of the average scintillation index (one for each hour of the day). A correlation analysis between the scintillation indices for each latitude was done for all latitudes. The results are shown in Figure 20 where the correlation coefficient is plotted as a function of latitude for each latitude interval. Smooth curves have been drawn through the points to facilitate interpretation of the graphs. The significance level of the correlation coefficient for 24 data points is .34 and is indicated by the horizontal line drawn through each curve. Consider the curve for the latitude interval 35°-40°. The observing station is at about 37° N latitude. If the scintillation activity is to be a minimum at the observers latitude, the scintillation index in the interval 35°-40° should not correlate well with the scintillation indices observed when the satellite is north or south of 37°. This is indeed the case. The more rapid decay of the correlation coefficient for latitudes north

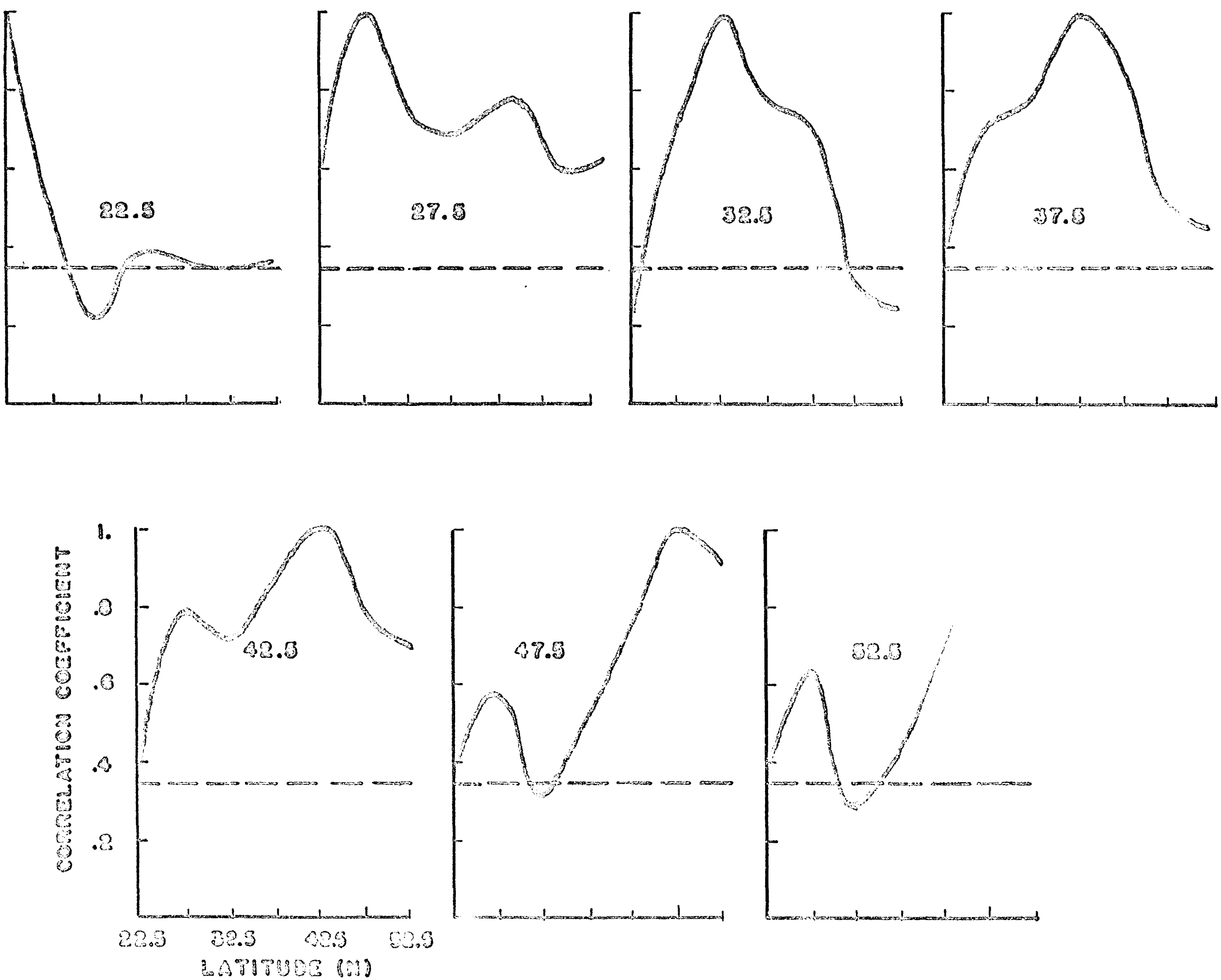

CORRELATION COEFFICIENT VS. LATITUDE

FIGURE 20

of 37° indicates a greater change in the scintillation index in the northly direction. The slower decay for latitudes south of 37° indicate a less intense change in the scintillation index in the southerly direction. These changes are significant since the significance level falls below the features discussed. The other curves may be interpreted in the same manner. All curves appear to show the existence of a minimum of scintillation activity at about 33° latitude and also show the north-south asymmetry about the observation station.

Lawrence and Martin have examined the seasonal variation in satellite scintillation for 3 month intervals centered on the solstices and equinoxes. The data were averaged over two hour intervals throughout the 24 hour day for each of the three month periods for all elevation angles. It is concluded that scintillation activity is strongest during a period centered on the autumnal equinox and weakest during a period centered on the vernal equinox. Chivers reports a maximum of the mean scintillation index for cosmic radiation at the equinoxes and a minimum at the solstices. Bolton et al. observe the opposite effect while Briggs and Dagg observe no seasonal variation. Thus the seasonal variation of star scintillation activity is not well understood at present. Consequently no comparison of seasonal variations of satellite scintillation and radio star scintillation can be made here.

Alexander has conducted a study of the variation of satellite scintillation with elevation angle at Williamsburg, Virginia. The scintillation index was averaged over five degree elevation intervals for all azimuth angles for 70 passes. It is concluded that maximum scintillation occurs near the horizon and decreases steadily as the elevation angle increases to 20°. Above this elevation the activity appears to level out at a minimum. A sharp increase in scintillation activity above 65° is attributed to poor statistics and the high apparent velocity of the satellite at high elevation angles; a phenomena which gives rise to an extremely rapid fading rate. A decrease in cosmic scintillation activity with increasing elevation angle, noted by all observers, is in general agreement with the results obtained by Alexander for satellite scintillation.

CONCLUSION

A correlation analysis of the data obtained indicates that there is no one-to-one correspondence between satellite and radio star scintillation activity. Because of the consistantly low values of the star scintillation index due mainly to the time at which observations were made, no general correspondence can be inferred. A comparison of published features of star scintillation activity and satellite studies made at the College of William and Mary shows the following features common to each:

1. Satellite scintillation, like radio star scintillation, is predominately a night time phenomena with maximum activity occurring around midnight. Observers in Canada and Australia see a secondary midday maximum in star scintillation which is in agreement with a similar maximum observed at Williamsburg for satellite scintillation.

2. A distinct variation of satellite scintillation activity with latitude is noted at Williamsburg. Activity is a minimum at the latitude of the observation station and increases markedly for position of the satellite north of the station. A smaller increase is observed when the satellite is south of the station. A similar latitude dependence is observed for radio star scintillations with greater activity at latitudes to the north of the observation station.

3. At Williamsburg a variation of satellite scintillation activity with elevation angle is observed. Maximum activity occurs near the horizon and decreases steadily as the elevation angle increases to 20°. Above 20° activity appears to level out to a steady minimum. This also is in general agreement with the elevation effect observed for radio star scintillation.

Since seasonal variation of radio star scintillation is not well understood, no comparison with seasonal variation of satellite scintillations reported at Williamsburg has been made. Although variations of radio star scintillation with the solar cycle have been published recently in the literature[16], there are at present no similar studies for satellite scintillation available. Latitudinal, diurnal, and elevation angle effects seem to indicate that there is good general correlation between radio star and satellite scintillation activity. Further investigations of seasonal effects and variation of scintillation phenomena with the solar cycle will provide a more complete basis for comparison of satellite and cosmic scintillation phenomena.

REFERENCES

1. Jansky, K. G., Proc. IRE 20, 1920 (1932)
2. Hey, J. S., Parsons, S. J. and Phillips, J. W., Nature 158, 234 (1946)
3. Smith, F. G., Nature 165, 422 (1950)
4. Little, G. C. and Lovell, A. C. B., Nature 165, 423 (1950)
5. Booker, H. G., Proc. IRE 46, 298 (1958)
6. Yeh, K. C. and Swenson, C. W., J. Geophys. Res. 64, 2281 (1959)
7. Lawrence, J. D., Jr., and Martin, J. D., J. Geophys. Res. 69, 1293 (1964)
8. Slee, O. B., Nature 181, 1610 (1958)
9. Parthasarathy, R. and Reid, G. C., Proc. IRE 47, 78 (1959)
10. Standards on Wave-Propagation. Definition of terms, 1950 Proc. IRE 38, 1264 (1950)
11. Aiken, A. C., "A Preliminary Study of Sunrise Effects in the D Region," Ionospheric Research Report No. 133, Penn. State Univ. (1960)
12. Nicholet, M. and Aikin, A. C., J. Geophys. Res. 65, 1469 (1960)
13. Gibson, J. J. and Waynick, A. H., Proc. IRE 47, 160 (1959)
14. Smith, E. K., "Worldwide Occurrence of Sporadic E," Natl. Bur. Standards Circular 582, (1957)

15. Martyn, D. F., Proc. IRE 47, 147 (1959)

16. Briggs, B. H., J. Atmos. Terr. Phys. 26, 1 (1964)

17. Ryle, M. and Vonberg, D. D., Proc. Roy. Soc., A193, 98 (1948)

18. Hollinger, J. P., Ph. D. Dissertation University of Virginia (1961)

19. Nyquist, H., Phys. Rev. 32, 110 (1928)

20. Bowhill, S. A., Penn. State Report No. 89 (1956)

21. Alexander, J. K., M. A. Thesis College of William and Mary (1962)

22. Martin, J. D., M. A. Thesis College of William and Mary (1963)

23. Lawrence, J. D., Ph. D. Dissertation University of Virginia (1960)

24. Chivers, H. J. A., J. Atmos. Terr. Phy. 19, 54 (1960)

25. Singleton, D. G., J. Atmos. Terr. Phy. 22, 219 (1961)

26. Dagg, M., J. Atmos. Terr. Phy. 10, 204 (1957)

27. Ryle, M. and Hewish, A., Monthly Notices of the Royal Astronomical Society 110, 384 (1950)

28. Little, C. G. and Maxwell, A., Phil. Mag. 42, 267 (1951)

29. Bolton, J. G., Slee, O. B., and Stanley, G. J., Austrian Journal of Physics, A6, 434 (1953)

30. Harrower, G. A., Canad. J. of Phy. 35, 512 (1957)

31. Briggs, B. H. and Parkin, I. A., J. Atmos. Terr. Phy. 25, 339 (1963)